

THE DEVELOPMENT OF A MATHEMATICAL MODEL AND A STUDY OF
ONE METHOD OF ORBIT ADJUST AND STATION KEEPING
GRAVITY-ORIENTED SATELLITES

By Curtiss C. Barrett

Goddard Space Flight Center
Greenbelt, Md.

NATIONAL AERONAUTICS AND SPACE ADMINISTRATION

For sale by the Clearinghouse for Federal Scientific and Technical Information
Springfield, Virginia 22151 - Price \$2.50

ABSTRACT

The differential equations of motion for a coupled two-body, gravity-oriented, satellite are derived in Part I. Each of the two bodies is assumed to be rigid. The satellite configuration is basically an x with a damper rod attached so that it is free to move constrained only by a spring damper mechanism in a plane fixed with respect to the x plane. This leads to a seven degree-of-freedom problem. A FORTRAN II digital program is included in Appendix D to provide a numerical solution for these equations.

In Part II one method of orbit adjust and station keeping is studied. The satellite parameters are chosen for a medium altitude (approximately 6000 nautical miles) orbit. A one pound thrust level and a misalignment angle of one degree are assumed for the station keeping thrusters. The results of the study show that a 0.01 orbit eccentricity change can be made in 40 days with tangential pulses of 40 seconds duration every 22.4 hours without causing satellite inversion. However, tangential pulsing requires sensing the satellite yaw angle and, a significant number of damper rod collisions, with mechanical stops placed at one radian on either side of the null position, resulted. These two problems are avoided by using radial pulses but, the eccentricity change is only 0.0057 after 40 days of correction.

CONTENTS

Abstract	ii
INTRODUCTION	1
I: DEVELOPMENT OF A MATHEMATICAL MODEL FOR A GRAVITY-ORIENTED SATELLITE	3
SATELLITE DESCRIPTION	3
REFERENCE COORDINATE SYSTEMS	3
Inertial Coordinate System	3
Geocentric Coordinate System	4
Attitude Reference System	4
Body Frame Reference System	4
Damper Rod Reference System	4
DERIVATION OF EQUATIONS OF MOTION	7
Translational Equations of Motion	7
Rotational Equations of Motion	8
METHOD OF SOLUTION	17
II: A STUDY OF ONE METHOD OF ORBIT ADJUST AND STATION KEEPING	18
SATELLITE ORBIT AND PARAMETERS	18
STEADY STATE DYNAMICS OF THE SATELLITE	18
SATELLITE RESPONSE TO AN IMPULSIVE TORQUE	19
THRUST PROGRAM	20
DISCUSSION OF RESULTS	23
CONCLUSIONS	24
References	25
Appendix A—List of Symbols	27
Appendix B—Elements Defining a Satellite Orbit	29
Appendix C—Gravitational Moments Generated by Earth Potential	33
Appendix D—A Gravity-Oriented Satellite Digital Program	37

THE DEVELOPMENT OF A MATHEMATICAL MODEL AND A STUDY OF ONE METHOD OF ORBIT ADJUST AND STATION KEEPING GRAVITY-ORIENTED SATELLITES*

by
Curtiss C. Barrett
Goddard Space Flight Center

INTRODUCTION

Spacecraft designers are currently faced with the problem of developing, at minimum cost, satellites with long lifetimes without sacrificing reliability. Many of these satellites will provide services which do not require precise attitude control, such as providing communications links and gathering meteorological data. The cost of these satellites can be greatly reduced by having one side always facing the earth. This, for example, eliminates the necessity of having directional control of television cameras or receiving and transmitting antennas. Gravity-gradient stabilization has this property, and it seems that reliability for long lifetimes is possible, since this is a passive technique.

The concept of gravity-gradient stabilization is not new. Roberson (Reference 1) attributes to Laplace the first recognition of this effect and its application in 1785 to the problem of the stability of the moon with one face always pointing toward the earth. This tendency of an elongated body to align itself with the local gravitational field can be made an actuation control source, if the satellite configuration is chosen so that the stable attitude in the gravitational field is the desired attitude. Any system based on this principle would require some method of damping oscillatory motion to be practical. Among the early investigators of gravity-gradient stabilization, Paul (Reference 2) showed that the librations of an extensible dumbbell satellite could be damped by dissipating energy through the vibration of an elastic material. About the same time, work was initiated at the Applied Physics Laboratory of Johns Hopkins University on connecting two masses by an elastic spring and energy-dissipating device, a concept which was later incorporated into the TRAAC satellite (Reference 3). Kamm (Reference 4) analyzed a satellite to which were hinged, with appropriate damping mechanisms, two long rods to provide three-axis damping of librations. Tinling and Merrick (Reference 5) showed that similar results could be obtained by a single damper rod positioned so as to cause satellite inertial asymmetry with respect to the orbital plane. It was

*Taken from a dissertation submitted at the Catholic University of America in partial fulfillment of the requirements for the degree of Master of Science.

shown that the necessary inertial properties could be obtained by erecting fixed rods in the form of an X with the payload at the center and a damper rod attached in the horizontal plane. This latter concept seems very promising and is currently being considered as a stabilization system for a number of future satellites.

The purpose of Part I of this paper is to analyze the motion of the coupled satellite in the presence of a central gravitational field. The orientation of the satellite is specified at any time by three translational coordinates, three rotational coordinates or attitude deviation angles, and an angle which locates the damper rod with respect to the main body of the satellite. These seven variables are derived in differential equation form.

Perturbing forces produced by the non-sphericity of the earth's gravity field and the presence of the sun and moon constantly act to remove the satellite from its desired orbit. Since gravity-oriented satellites are expected to endure long lifetimes precisely on station, station keeping becomes a requirement. Thruster misalignment is typical of the many problems to be considered and may be even more critical for gravity-oriented satellites because of the large moments of inertia involved.

Part II of this paper presents the results of a study to find a thrust program capable of station keeping a gravity-oriented satellite. Disturbing torques considered are those due to thruster misalignment and those arising naturally from variation of the radius vector in elliptic orbits of small eccentricity.

In Appendix D is a Fortran II digital program which provides the numerical solution to the equations derived in Part I. This program was used in the study made in Part II.

SATELLITE DESCRIPTION

The inertial properties of the satellite may be varied by changing the angle of the x and by varying the angle between the damper rod rotation plane and the x plane. For the purpose of this report these two quantities will be considered as constants.

REFERENCE COORDINATE SYSTEMS

Inertial Coordinate System

X In equatorial plane, along line of equinoxes toward vernal equinox,
Y In equatorial plane, normal to X,



and

Z Along earth's spin axis, toward North Pole.

Geocentric Coordinate System

The geocentric coordinates, like the inertial coordinates, are referenced to the center of the earth (Figure 3). The coordinate axes are:

X_c Outward along earth-satellite radius vector,

Y_c In orbital plane, parallel to satellite height circle tangent,

and

Z_c Parallel to satellite meridian circle tangent.

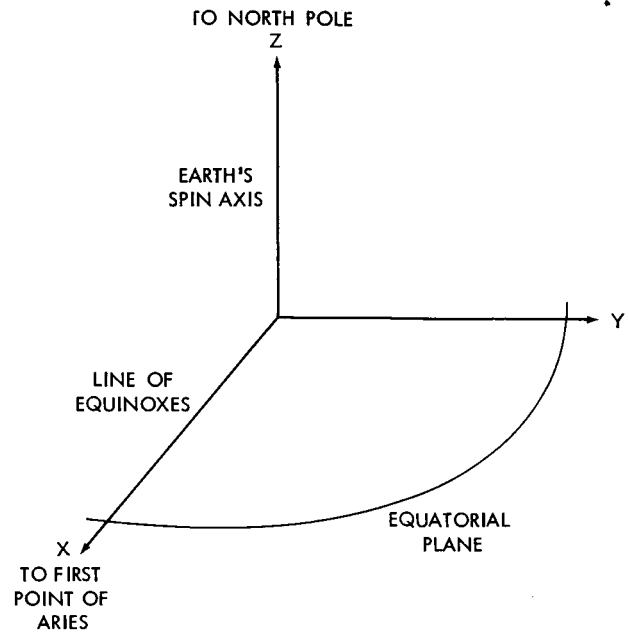


Figure 2—Inertial reference system.

Attitude Reference System

The attitude coordinates are referenced to the satellite (Figure 4). The coordinate axes are:

X_0 Outward along earth-satellite radius vector,

Y_0 Tangent to satellite orbit path, same sense as vehicle motion,

and

Z_0 Normal to satellite orbit plane.

Body Frame Reference System

The body frame is referenced to the plane of the x , with the frame center as the origin (Figure 5). The coordinate axes are:

x_b In plane of rods, bisecting smaller angle made by rods,

y_b In plane of rods, normal to x_b ,

and

z_b Normal to plane of rods.

Damper Rod Reference System

The damper rod is referenced to the rod hinge with the hinge point as origin (Figure 6). The coordinate axes are:

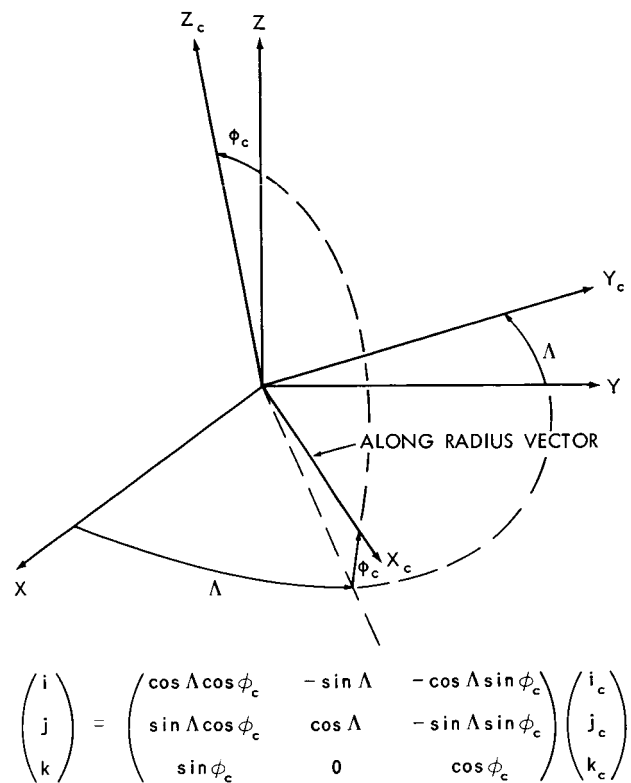
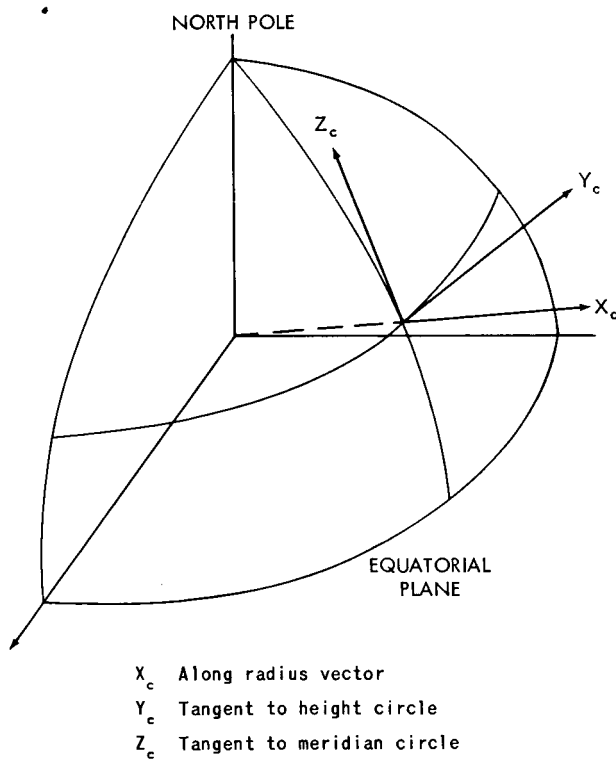


Figure 3—Geocentric coordinate system, (a) Geocentric reference frame, shown with satellite origin for clarity; rotational properties are not affected, (b) Rotational transformation of coordinates from geocentric to inertial reference frame.

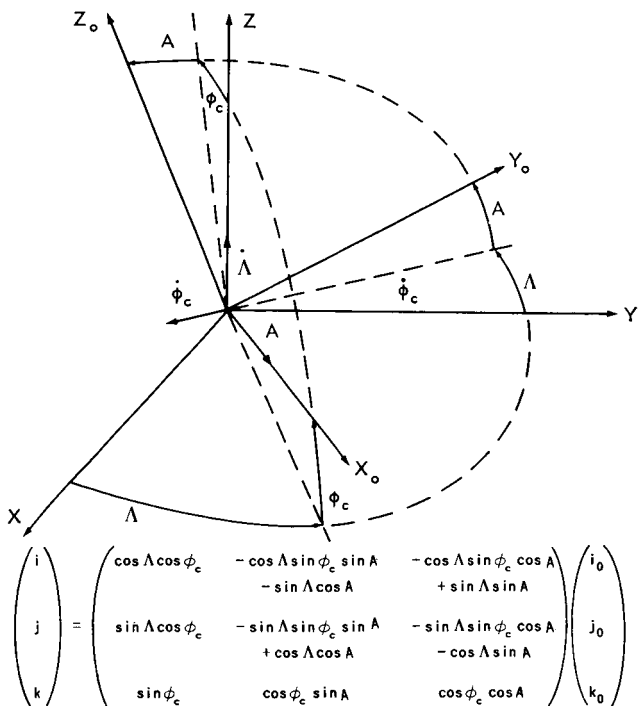
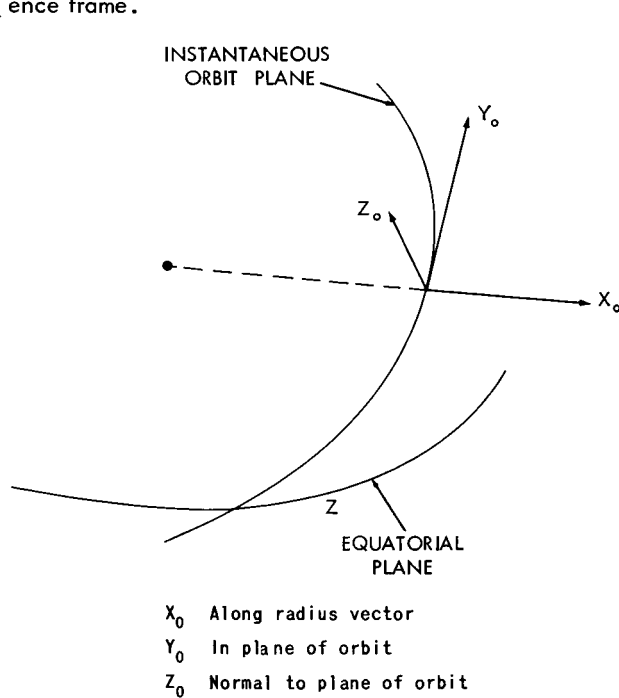
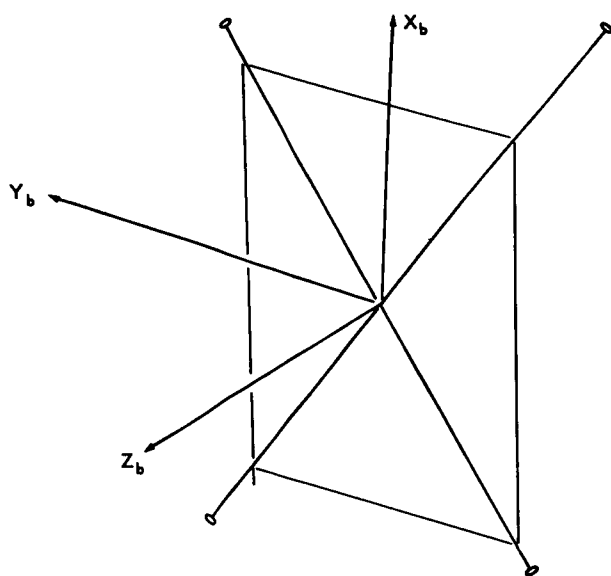


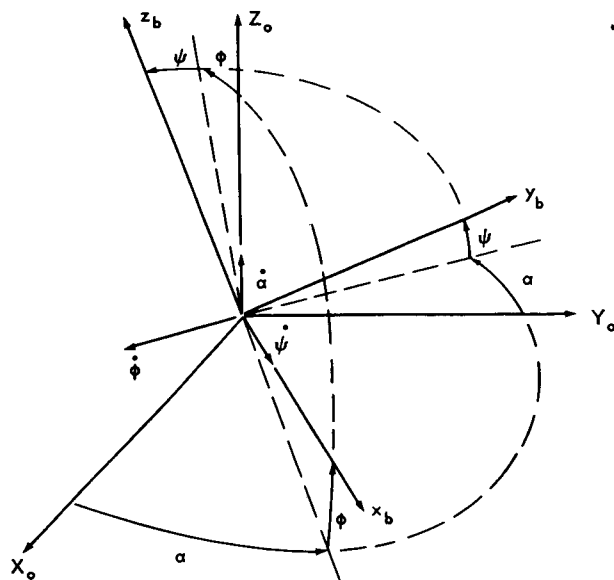
Figure 4—Attitude coordinate system, (a) Orbit or attitude reference frame, shown with earth center origin for clarity; rotational properties are not affected, (b) Rotational transformation of coordinates from the attitude to the inertial reference frame.



$X_b - Y_b$ Plane = Plane of "X"

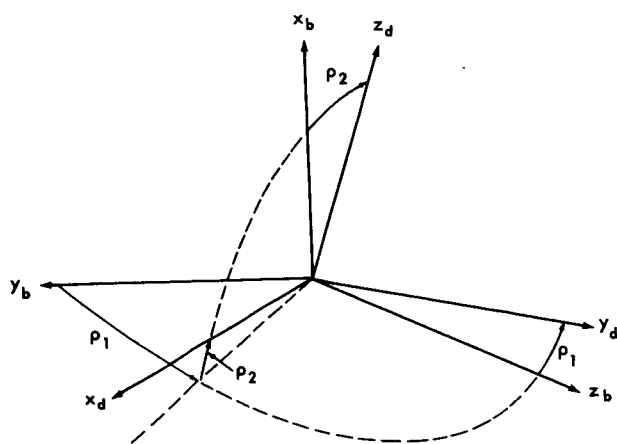
Z_b Normal to plane of "X"

X_b Bisects the smallest angle of the "X"



$$\begin{pmatrix} i_0 \\ j_0 \\ k_0 \end{pmatrix} = \begin{pmatrix} \cos \alpha \cos \phi & -\cos \alpha \sin \phi \sin \psi & -\cos \alpha \sin \phi \cos \psi \\ & -\sin \alpha \cos \psi & +\sin \alpha \sin \psi \\ \sin \alpha \cos \phi & -\sin \alpha \sin \phi \sin \psi & -\sin \alpha \sin \phi \cos \psi \\ & +\cos \alpha \cos \psi & -\cos \alpha \sin \psi \\ \sin \phi & \cos \phi \sin \psi & \cos \phi \cos \psi \end{pmatrix} \begin{pmatrix} i_b \\ j_b \\ k_b \end{pmatrix}$$

Figure 5—Body frame coordinate system, (a) Body reference frame, (b) Rotational transformation of coordinates from body to attitude reference frame.



$$\begin{pmatrix} i_b \\ j_b \\ k_b \end{pmatrix} = \begin{pmatrix} \sin \rho_2 & 0 & \cos \rho_2 \\ \cos \rho_2 \cos \rho_1 & -\sin \rho_1 & -\sin \rho_2 \cos \rho_1 \\ \cos \rho_2 \sin \rho_1 & \cos \rho_1 & -\sin \rho_2 \sin \rho_1 \end{pmatrix} \begin{pmatrix} i_d \\ j_d \\ k_d \end{pmatrix}$$

Figure 6—Rotational transformation of coordinates from damper rod to body reference frame.

X_d Lying along rod length,

Y_d Axis about which rod rotates,

and

Z_d Defined by $T_{d \rightarrow b}$ when ρ_1 and ρ_2 vanish,

where the transformation is

$$\begin{pmatrix} T_{d \rightarrow b} \end{pmatrix} = \begin{pmatrix} 0 & 0 & 1 \\ 1 & 0 & 0 \\ 0 & 1 & 0 \end{pmatrix}.$$

In Figures 4(b), 5(b), and 6, transformation matrices accompany the diagrams. At times in the report these matrices will be referred to merely as $\begin{pmatrix} T_{\alpha \rightarrow \beta} \end{pmatrix}$ when they represent an obvious transformation of a vector from its

representation in the $[X, Y, Z]_a$ system to representation in the $[X, Y, Z]_\beta$ system, where a and β are coordinate identification subscripts.

DERIVATION OF EQUATIONS OF MOTION

Orientation of the satellite is given at any time by the following variables:

- (1) The three translational coordinates, which fix the satellite position with respect to a standard inertial coordinate system.
- (2) The three rotational coordinates or attitude deviation angles, designating the satellite attitude as measured in an orbital coordinate system or attitude reference system.
- (3) The angle made by the damper rod constrained to rotate in a plane fixed with respect to the main body (damper rod angle).

Translational Equations of Motion

When viewed in inertial spherical coordinates, the satellite position is determined by the parameters r , Λ , and ϕ_c . Associated with this triplet are both a velocity vector

$$\vec{V} = [V_r, V_\Lambda, V_{\phi_c}]$$

and an acceleration vector

$$\vec{A} = [A_r, A_\Lambda, A_{\phi_c}] = \left[\frac{F_r}{m}, \frac{F_\Lambda}{m}, \frac{F_{\phi_c}}{m} \right],$$

where m represents the satellite mass and F_r , F_Λ , and F_{ϕ_c} are the external forces acting on the system.

When expressed in spherical coordinates, the components of \vec{V} and \vec{A} are

$$V_r = \dot{r}, \quad (1a)$$

$$V_\Lambda = r \dot{\Lambda} \cos \phi_c, \quad (1b)$$

$$V_{\phi_c} = r \dot{\phi}_c, \quad (1c)$$

and

$$A_r = \frac{F_r}{m} = \ddot{r} - r \dot{\Lambda}^2 \cos^2 \phi_c - r \dot{\phi}_c^2, \quad (2a)$$

$$A_{\Lambda} = \frac{F_{\Lambda}}{m} = \frac{1}{r \cos \phi_c} \frac{d}{dt} \left(r^2 \dot{\Lambda} \cos^2 \phi_c \right), \quad (2b)$$

$$A_{\phi_c} = \frac{F_{\phi_c}}{m} = \frac{1}{r} \frac{d}{dt} \left(r^2 \dot{\phi}_c \right) + r \dot{\Lambda}^2 \sin \phi_c \cos \phi_c. \quad (2c)$$

Rewriting Equations 2 in terms of the highest derivative results in

$$\ddot{r} = \left(r \dot{\Lambda}^2 \cos^2 \phi_c + r \dot{\phi}_c^2 \right) + \frac{F_r}{m}, \quad (3a)$$

$$\frac{d}{dt} \left(r^2 \dot{\Lambda} \cos^2 \phi_c \right) = \frac{F_{\Lambda}}{m} (r \cos \phi_c), \quad (3b)$$

$$\frac{d}{dt} \left(r^2 \dot{\phi}_c \right) = r \left(\frac{F_{\phi_c}}{m} - r \dot{\Lambda}^2 \sin \phi_c \cos \phi_c \right). \quad (3c)$$

Successive integrations of Equations 3 will lead to the determination of the variables r , Λ , and ϕ_c . In the present form the equations permit the inclusion of any external force functions known to be acting on the system.

Any second-order ordinary differential equation, when integrated, will require two constants of integration. For the definite integrals occurring here, these are the *initial conditions*, which must be determined by other means. The Runge-Kutta method of numerical integration, utilized in this report, requires knowledge of the dependent variable and its first derivative at one point in order to generate a point-to-point solution for each equation. The total of six initial conditions may be obtained (as indicated in Appendix B) by specifying six orbital elements, which may then be used to compute the initial conditions. The procedure adopted for computer solution is to designate a set of orbital elements, solve for the desired constants, and then integrate the equations by quadrature to obtain the time-varying coordinate parameters. Also shown in Appendix B are equations necessary for computing new orbital elements from the integrated variables. These orbital changes would be caused by noncentral forces.

Rotational Equations of Motion

Once the satellite's position in space is known, it then remains to determine its attitude with respect to a known coordinate system, chosen here to be the attitude reference system shown in Figure 4. Such a determination is made easier by the fact that, to an excellent approximation, the angular motion of the vehicle about its center of mass can be completely decoupled from its angular motion in orbit about the earth. Consequently, the basic equation of attitude motion is simply that the time rate of change of angular momentum \vec{H} is equal to the applied external torque. Considering that the body reference system $[x_b, y_b, z_b]$ for which the angular momentum is defined is itself rotating with respect to the previously noted inertial reference system with angular velocity

$\vec{\Omega} = [\Omega_{x_b}, \Omega_{y_b}, \Omega_{z_b}]$, the time rate of change of \vec{H} , as seen by an observer at the origin of the inertial system, is expressed by

$$\dot{\vec{H}}_c = \dot{\vec{H}} + \vec{\Omega} \times \vec{H}, \quad (4)$$

where

$$\dot{\vec{H}} = \begin{pmatrix} I_{xx} & I_{xy} & I_{xz} \\ I_{xy} & I_{yy} & I_{yz} \\ I_{xz} & I_{yz} & I_{zz} \end{pmatrix} \begin{pmatrix} \Omega_{x_b} \\ \Omega_{y_b} \\ \Omega_{z_b} \end{pmatrix}$$

(Reference 6).

For the coupled satellite, Equation 4 may be applied to both the main frame and the damper rod, leading to

$$\frac{d}{dt} \left[\begin{pmatrix} I_{xx} & I_{xy} & I_{xz} \\ I_{xy} & I_{yy} & I_{yz} \\ I_{xz} & I_{yz} & I_{zz} \end{pmatrix} \begin{pmatrix} \Omega_{x_b} \\ \Omega_{y_b} \\ \Omega_{z_b} \end{pmatrix} \right] + \begin{pmatrix} \Omega_{y_b} H_{z_b} - \Omega_{z_b} H_{y_b} \\ \Omega_{z_b} H_{x_b} - \Omega_{x_b} H_{z_b} \\ \Omega_{x_b} H_{y_b} - \Omega_{y_b} H_{x_b} \end{pmatrix} = \begin{pmatrix} M_{x_b} + R_{x_b} \\ M_{y_b} + R_{y_b} \\ M_{z_b} + R_{z_b} \end{pmatrix} \quad (5)$$

for the main frame, and

$$I_r \dot{\Omega}_{x_d} = M_{x_d} + R_{x_d}, \quad (6a)$$

$$I_\ell \dot{\Omega}_{y_d} + (I_r - I_\ell) \Omega_{z_d} \Omega_{x_d} = M_{y_d} + R_{y_d}, \quad (6b)$$

and

$$I_\ell \dot{\Omega}_{z_d} - (I_r - I_\ell) \Omega_{x_d} \Omega_{y_d} = M_{z_d} + R_{z_d}, \quad (6c)$$

for the hinged rod. Note that I_r is about the rod axis, and I_ℓ is normal to the axis.

In Equations 5 and 6 the term \vec{M} represents external torques on the configuration, while \vec{R} represents the internal reaction torque(s) between the two sections of the vehicle. It follows that since the rod and frame are connected at all times, the reaction torques on the two sections are equal in magnitude although opposite in direction. This may be expressed as

$$\begin{pmatrix} R_{x_b} \\ R_{y_b} \\ R_{z_b} \end{pmatrix} = \begin{pmatrix} T \\ T \\ T \end{pmatrix}_{d \rightarrow b} \begin{pmatrix} R_{x_d} \\ R_{y_d} \\ R_{z_d} \end{pmatrix} \quad (7)$$

The spring-damper mechanism acts, as mentioned earlier, to damp the rod in its rotation about the Y_d axis. This restoring torque, denoted by M_{SD} , is equivalent to the reaction torque component R_{y_d} ; if Equations 6a to 6c are rearranged to solve for R_{x_d} , R_{y_d} and R_{z_d} , respectively, the results are

$$R_{x_d} = I_r \dot{\Omega}_{x_d} - M_{x_d}, \quad (8a)$$

$$R_{y_d} = M_{SD}, \quad (8b)$$

and

$$R_{z_d} = I_\ell \dot{\Omega}_{z_d} - (I_r - I_\ell) \Omega_{x_d} \Omega_{y_d} - M_{z_d} \quad (8c)$$

Were the damper rod to be confined rigidly to the Y_d axis, the transformation of angular velocity $\vec{\Omega}$ from the body coordinate system to the rod coordinate system could be expressed simply as $\vec{\Omega}_d = \begin{pmatrix} T \\ b \rightarrow d \end{pmatrix} \vec{\Omega}_b$. However, the motion $\dot{\rho}_2$ of the rod induced relative to the Y_d axis by the spring coupling must be considered in the transformation. This is seen to lead to the revised expression

$$\begin{pmatrix} \Omega_{x_d} \\ \Omega_{y_d} + \dot{\rho}_2 \\ \Omega_{z_d} \end{pmatrix} = \begin{pmatrix} T \\ b \rightarrow d \end{pmatrix} \begin{pmatrix} \Omega_{x_b} \\ \Omega_{y_b} \\ \Omega_{z_b} \end{pmatrix} \quad (9)$$

Formal differentiation of Equation 9 under the rules of matrix algebra yields

$$\begin{pmatrix} \dot{\Omega}_{x_d} \\ \dot{\Omega}_{y_d} + \dot{\rho}_2 \\ \dot{\Omega}_{z_d} \end{pmatrix} = \left[\frac{d}{dt} \begin{pmatrix} T \\ b \rightarrow d \end{pmatrix} \right] \begin{pmatrix} \Omega_{x_b} \\ \Omega_{y_b} \\ \Omega_{z_b} \end{pmatrix} + \begin{pmatrix} T \\ b \rightarrow d \end{pmatrix} \begin{pmatrix} \dot{\Omega}_{x_b} \\ \dot{\Omega}_{y_b} \\ \dot{\Omega}_{z_b} \end{pmatrix} \quad (10)$$

Note that in the actual differentiation of the matrix $\begin{pmatrix} T \\ b \rightarrow d \end{pmatrix}$ the angle ρ_1 made by the plane of rotation of the rod with the X-frame plane is a constant, and so all $d/dt (\rho_1)$ terms vanish.

At this point it should be explained what is desired: a functional relation between the angular velocity vector $\vec{\Omega}_b = [\Omega_{x_b}, \Omega_{y_b}, \Omega_{z_b}]$ and known quantities. This expression, in the form of a differential equation or set of equations, will then be numerically integrated to determine the angular velocity components. However, these are in turn functionally related to the derivatives of the attitude deviation angles α , ϕ , and ψ ; thus all that remains is to integrate the resulting set of equations. In this manner the attitude deviation angles will have been determined.

To accomplish this task, Equation 8 is first rewritten in terms of $\vec{\Omega}_b$ and $\dot{\vec{\Omega}}_b$; these latter terms come from Equations 9, 10a, and 10c. It should be pointed out that Equation 10b is not

used at the present time. The revised Equation 8 is substituted for the vector $\begin{bmatrix} R_{x_d}, R_{y_d}, R_{z_d} \end{bmatrix}$ in Equation 7. The right-hand term in Equation 7 then replaces $\begin{bmatrix} R_{x_b}, R_{y_b}, R_{z_b} \end{bmatrix}$ in Equation 5; the new equation results.

$$\begin{pmatrix} I_{xx} & I_{xy} & I_{xz} \\ I_{xy} & I_{yy} & I_{yz} \\ I_{xz} & I_{yz} & I_{zz} \end{pmatrix} \begin{pmatrix} \dot{\Omega}_{x_b} \\ \dot{\Omega}_{y_b} \\ \dot{\Omega}_{z_b} \end{pmatrix} + \begin{pmatrix} \Omega_{y_b} H_{z_b} - \Omega_{z_b} H_{y_b} \\ \Omega_{z_b} H_{x_b} - \Omega_{x_b} H_{z_b} \\ \Omega_{x_b} H_{y_b} - \Omega_{y_b} H_{x_b} \end{pmatrix} = \begin{pmatrix} M_{x_b} \\ M_{y_b} \\ M_{z_b} \end{pmatrix} + \begin{pmatrix} f_1(\vec{\Omega}_b, \dot{\vec{\Omega}}_b) \\ f_2(\vec{\Omega}_b, \dot{\vec{\Omega}}_b) \\ f_3(\vec{\Omega}_b, \dot{\vec{\Omega}}_b) \end{pmatrix} \quad (11)$$

Comparison with Equation 5 reveals that the term $(d/dt)[I_{a\beta}]$ is assumed to be of the form

$$\begin{pmatrix} 0 & 0 & 0 \\ 0 & 0 & 0 \\ 0 & 0 & 0 \end{pmatrix} = 0.$$

The terms f_1 , f_2 , and f_3 are written here to show that a functional relationship exists in terms of the quantities $\vec{\Omega}_b$ and $\dot{\vec{\Omega}}_b$. The actual expansions are not included here, since they are merely an intermediate step in the solution of the problem.

Equation 11 may be rearranged so that all derivatives of the angular velocity appear on one side of the equation; this is represented by

$$\begin{pmatrix} \dot{\Omega}_{x_b} \\ \dot{\Omega}_{y_b} \\ \dot{\Omega}_{z_b} \end{pmatrix} = \frac{1}{\Delta} \begin{pmatrix} K_{xx} & K_{xy} & K_{xz} \\ K_{xy} & K_{yy} & K_{yz} \\ K_{xz} & K_{yz} & K_{zz} \end{pmatrix} \begin{pmatrix} \delta_{x_b} \\ \delta_{y_b} \\ \delta_{z_b} \end{pmatrix}, \quad (12)$$

where

$$\Delta = \det \begin{vmatrix} J_{xx} & J_{xy} & J_{xz} \\ J_{xy} & J_{yy} & J_{yz} \\ J_{xz} & J_{yz} & J_{zz} \end{vmatrix},$$

and the matrix elements $K_{ij} = (\alpha_{ij})$ (cofactor of J_{ij}), where i, j are summation indices over elements x, y, z and with

$$\alpha_{xx} = +1,$$

$$\alpha_{xy} = -1 ,$$

$$\alpha_{xz} = +1 ,$$

$$\alpha_{yy} = +1 ,$$

$$\alpha_{yz} = -1 ,$$

and

$$\alpha_{zz} = +1 .$$

The terms J_{ij} are defined as

$$J_{xx} = I_{xx} + I_\ell \cos^2 \rho_2 ,$$

$$J_{yy} = I_{yy} + I_\ell \sin^2 \rho_2 \cos^2 \rho_1 ,$$

$$J_{zz} = I_{zz} + I_\ell \sin^2 \rho_2 \sin^2 \rho_1 ,$$

$$J_{xy} = I_{xy} - I_\ell \sin \rho_2 \cos \rho_2 \cos \rho_1$$

$$J_{xz} = I_{xz} - I_\ell \sin \rho_2 \cos \rho_2 \sin \rho_1 ,$$

and

$$J_{yz} = I_{yz} + I_\ell \sin^2 \rho_2 \sin \rho_1 \cos \rho_1 ,$$

and the elements are

$$\delta_{x_b} = M_{x_b} + M_{x_d} \sin \rho_2 + M_{z_d} \cos \rho_2 - \left(\Omega_{y_b} H_{z_b} - \Omega_{z_b} H_{y_b} \right) - P \cos \rho_2 ,$$

$$\delta_{y_b} = M_{y_b} + M_{x_d} \cos \rho_2 \cos \rho_1 + M_{SD} \sin \rho_1 - M_{z_d} \sin \rho_2 \cos \rho_1 - \left(\Omega_{z_b} H_{x_b} - \Omega_{x_b} H_{z_b} \right) + P \sin \rho_2 \cos \rho_1 ,$$

and

$$\delta_{z_b} = M_{z_b} + M_{x_d} \cos \rho_2 \sin \rho_1 - M_{SD} \cos \rho_1 - M_{z_d} \sin \rho_2 \sin \rho_1 - \left(\Omega_{x_b} H_{y_b} - \Omega_{y_b} H_{x_b} \right) + P \sin \rho_2 \sin \rho_1 ,$$

where $P = I_\ell \Omega_{x_d} (\Omega_{y_d} - \dot{\rho}_2)$. Since the moment of inertia of the damper rod about its own axis is considerably less than its moment of inertia normal to the axis, the I_r terms have been dropped. It might also be noted that the $\vec{\delta}_b$ vector terms are still expressed as functions of moments and angular velocities referred to the rod coordinate system. This is merely a more convenient way of writing out the terms, as representation purely in terms of body coordinates makes the expressions excessively long.

The gravitational moment components referred to the frame coordinates and to the rod coordinates are (from Appendix C):

$$M_{x_b} = -\frac{3\mu}{r^3} \left[(I_{yy} - I_{zz}) a_2 a_3 + I_{xy} a_1 a_3 - I_{xz} a_1 a_2 + I_{yz} (a_3^2 - a_2^2) \right],$$

$$M_{y_b} = -\frac{3\mu}{r^3} \left[(I_{zz} - I_{xx}) a_1 a_3 - I_{xy} a_2 a_3 + I_{xz} (a_1^2 - a_3^2) + I_{yz} a_1 a_2 \right],$$

$$M_{z_b} = -\frac{3\mu}{r^3} \left[(I_{xx} - I_{yy}) a_1 a_2 + I_{xy} (a_2^2 - a_1^2) + I_{xz} a_2 a_3 - I_{yz} a_1 a_3 \right],$$

$$M_{x_d} = 0,$$

$$M_{y_d} = -\frac{3\mu}{r^3} I_\ell b_1 b_3,$$

and

$$M_{z_d} = \frac{3\mu}{r^3} I_\ell b_1 b_2,$$

where

$$a_1 = \cos \alpha \cos \phi,$$

$$a_2 = -\cos \alpha \sin \phi \sin \psi - \sin \alpha \cos \psi,$$

$$a_3 = -\cos \alpha \sin \phi \cos \psi + \sin \alpha \sin \psi,$$

$$b_1 = a_1 \sin \rho_2 + a_2 \cos \rho_2 \cos \rho_1 + a_3 \cos \rho_2 \sin \rho_1,$$

$$b_2 = -a_2 \sin \rho_1 + a_3 \cos \rho_1,$$

and

$$b_3 = a_1 \cos \rho_2 - a_2 \sin \rho_2 \cos \rho_1 - a_3 \sin \rho_2 \sin \rho_1.$$

Inspection of Equation 12 reveals that the only unspecified terms remaining are values of ρ_2 and $\dot{\rho}_2$. These values may be determined by considering Equations 6b and 10b, both of which have not yet been used:

$$I_\ell \dot{\Omega}_{y_d} - I_\ell \Omega_{z_d} \Omega_{x_d} = M_{y_d} + M_{SD}, \quad (6b)$$

$$\dot{\Omega}_{y_d} = -\dot{\Omega}_{y_b} \sin \rho_1 + \dot{\Omega}_{z_b} \cos \rho_1 - \ddot{\rho}_2. \quad (10b)$$

Elimination of $\dot{\Omega}_{y_d}$ between the two equations results in

$$\ddot{\rho}_2 = -\dot{\Omega}_{y_b} \sin \rho_1 + \dot{\Omega}_{z_b} \cos \rho_1 - \Omega_{z_d} \Omega_{x_d} - \frac{M_{y_d} + M_{SD}}{I_\ell} . \quad (13)$$

Numerical integration of Equation 13 will produce the term $\dot{\rho}_2$; a successive integration then yields the value of ρ_2 , one of the seven system parameters.

Integration of Equation 12 similarly generates the terms $[\Omega_{x_b}, \Omega_{y_b}, \Omega_{z_b}]$, from which it is desired to develop the attitude deviation angles α , ϕ , and ψ . However, the vector $\vec{\Omega}_b$ is referred to the inertial frame and may be seen as compounded of both motion of the body relative to the attitude coordinate system and motion directly attributable to the motion of the attitude system itself. This latter motion must be subtracted from the inertial rotation rate to represent the relative motion directly related to the attitude deviation angles. The procedure for this is as follows:

Figure 4b reveals that the angular velocity vectors \dot{A} , $\dot{\Lambda}$, and $\dot{\phi}_c$ of the attitude reference coordinates with respect to the inertial frame have components in the attitude reference frame of

$$\begin{aligned} \xi_{x_0} &= \dot{A} + \dot{\Lambda} \sin \phi_c , \\ \xi_{y_0} &= -\dot{\phi}_c \cos A + \dot{\Lambda} \cos \phi_c \sin A , \\ \xi_{z_0} &= \dot{\phi}_c \sin A + \dot{\Lambda} \cos \phi_c \cos A . \end{aligned} \quad (14)$$

Since the azimuth angle A is defined as $A = \arctan(\dot{\phi}_c / \dot{\Lambda} \cos \phi_c)$, it follows that

$$\dot{A} = \frac{(\dot{\Lambda} \cos \phi_c) \ddot{\phi}_c - \dot{\phi}_c (\ddot{\Lambda} \cos \phi_c - \dot{\Lambda} \dot{\phi}_c \sin \phi_c)}{\dot{\phi}_c^2 + \dot{\Lambda}^2 \cos^2 \phi_c} ,$$

or

$$\dot{A} = \frac{V_\Lambda r \ddot{\phi}_c - V_{\phi_c} (r \ddot{\Lambda} \cos \phi_c - r \dot{\Lambda} \dot{\phi}_c \sin \phi_c)}{V_\Lambda^2 + V_{\phi_c}^2} . \quad (15)$$

In Equations 2 the spherical coordinate functions are expressed in terms of the external forces F_r , F_Λ , F_{ϕ_c} . Using these latter terms, Equation 15 becomes

$$\dot{A} = \left[\frac{V_\Lambda F_{\phi_c} - V_{\phi_c} F_\Lambda}{m(V_\Lambda^2 + V_{\phi_c}^2)} - \dot{\Lambda} \sin \phi_c \right] , \quad (16)$$

while Equation 14 now takes the form

$$\xi_{x_0} = \frac{V_\Lambda F_{\phi_c} - V_{\phi_c} F_\Lambda}{m(V_\Lambda^2 + V_{\phi_c}^2)} ,$$

$$\xi_{y_0} = 0 , \quad (17)$$

and

$$\xi_{z_0} = \frac{1}{r} \left(v_A \cos A + v_{\phi_c} \sin A \right) .$$

The term ξ_{y_0} is equal to 0, since all rotation occurs about the axis from the earth through the satellite and the axis normal to the orbit plane.

With the integrated Equation 12 providing values for Ω_{x_b} , Ω_{y_b} , and Ω_{z_b} and utilizing Figure 5, it follows that

$$\begin{aligned} \Omega_{x_b} &= \dot{\alpha} \sin \phi + \dot{\psi} + \xi_{x_b} , \\ \Omega_{y_b} &= \dot{\alpha} \cos \phi \sin \psi - \dot{\phi} \cos \psi + \xi_{y_b} , \end{aligned} \quad (18)$$

and

$$\Omega_{z_b} = \dot{\alpha} \cos \phi \cos \psi + \dot{\phi} \sin \psi + \xi_{z_b} .$$

However, $\vec{\xi}_b$ is related to $\vec{\xi}_0$ by the transformation matrix

$$\begin{pmatrix} \xi_{x_b} \\ \xi_{y_b} \\ \xi_{z_b} \end{pmatrix} = \begin{pmatrix} \mathbf{T} \\ 0 \rightarrow b \end{pmatrix} \begin{pmatrix} \xi_{x_0} \\ \xi_{y_0} \\ \xi_{z_0} \end{pmatrix} , \quad (19)$$

which yields the equations

$$\begin{aligned} \dot{\alpha} &= \frac{1}{\cos \phi} \left[\left(\Omega_{y_b} - \xi_{y_b} \right) \sin \psi + \left(\Omega_{z_b} - \xi_{z_b} \right) \cos \psi \right] , \\ \dot{\phi} &= - \left(\Omega_{y_b} - \xi_{y_b} \right) \cos \psi + \left(\Omega_{z_b} - \xi_{z_b} \right) \sin \psi , \end{aligned} \quad (20)$$

and

$$\dot{\psi} = \Omega_{x_b} - \xi_{x_b} - \dot{\alpha} \sin \phi ,$$

where all terms on the right hand side will be initially specified. Consequently, numerical integration of Equation 20 will produce the attitude deviation angles needed to specify the vehicle orientation.

The damper rod is limited in its plane of rotation by stops placed symmetrically with respect to the Y_d -axis. When the rod collides with these stops, momentum and energy exchange between

the main body and the rod will result. Assuming both total energy and total momentum to be conserved, the relative velocity between the main body and the rod after collision is equal in magnitude but opposite in sign to the velocity before collision. This can be shown as follows. Let

$$\begin{aligned} L_{xx} &= I_{xx} + I_\ell \cos^2 \rho_2 , \\ L_{yy} &= I_{yy} + I_\ell (\sin^2 \rho_1 + \sin^2 \rho_2 \cos^2 \rho_1) , \\ L_{zz} &= I_{zz} + I_\ell (\cos^2 \rho_1 + \sin^2 \rho_2 \sin^2 \rho_1) , \\ L_{xy} &= I_{xy} - I_\ell \sin \rho_2 \cos \rho_2 \cos \rho_1 , \\ L_{xz} &= I_{xz} - I_\ell \sin \rho_2 \cos \rho_2 \sin \rho_1 , \end{aligned}$$

and

$$L_{yz} = I_{yz} - I_\ell \cos^2 \rho_2 \sin \rho_1 \cos \rho_1 .$$

Then the total kinetic energy of both bodies is given by

$$\begin{aligned} T_T &= \frac{1}{2} L_{xx} \Omega_{x_b}^2 + \frac{1}{2} L_{yy} \Omega_{y_b}^2 + \frac{1}{2} L_{zz} \Omega_{z_b}^2 + L_{xy} \Omega_{x_b} \Omega_{y_b} + L_{xz} \Omega_{x_b} \Omega_{z_b} + L_{yz} \Omega_{y_b} \Omega_{z_b} \\ &\quad + \dot{\rho}_2 I_\ell (\Omega_{y_b} \sin \rho_1 - \Omega_{z_b} \cos \rho_1) + \frac{1}{2} \dot{\rho}_2^2 I_\ell , \end{aligned} \quad (21)$$

and the total angular momentum of both bodies is given by

$$\begin{pmatrix} H_{T_x} \\ H_{T_y} \\ H_{T_z} \end{pmatrix} = \begin{pmatrix} L_{xx} & L_{xy} & L_{xz} \\ L_{xy} & L_{yy} & L_{yz} \\ L_{xz} & L_{yz} & L_{zz} \end{pmatrix} \begin{pmatrix} \Omega_{x_b} \\ \Omega_{y_b} \\ \Omega_{z_b} \end{pmatrix} + \dot{\rho}_2 I_\ell \begin{pmatrix} 0 \\ \sin \rho_1 \\ -\cos \rho_1 \end{pmatrix} . \quad (22)$$

Solving Equations 22 for Ω_{x_b} , Ω_{y_b} , and Ω_{z_b} in terms of $\dot{\rho}_2$ and substituting into Equation 21 gives

$$\dot{\rho}_2 = \pm \sqrt{\text{constant}} . \quad (23)$$

Obviously, one of the values of $\dot{\rho}_2$ given by Equation 23 must be the value when no collision takes place. It therefore follows when a collision takes place that

$$\dot{\rho}_2 \text{ (after collision)} = -\dot{\rho}_2 \text{ (before collision)} . \quad (24)$$

The values of Ω_{x_b} , Ω_{y_b} , and Ω_{z_b} after the collision can then be found by substituting the new value of $\dot{\rho}_2$ into Equations (22) and solving simultaneously.

METHOD OF SOLUTION

At this point, analysis of the system motion is completed, with the satellite position in space determined by integrating Equation (3), the body orientation determined by integrating Equation (20), and the angle made by the damper rod determined by integrating Equation (13). The motion of the various elements will be continuous and differentiable, except when the damper rod collides with one of the stops. This nondifferentiability may be circumvented by utilizing Equations (21) and (22) whenever a collision occurs. Appendix D provides a means of finding numerical solutions to these equations.

In the present form the derived equations of motion are functions of general external forces, although the gravitational moments derived in Appendix C are considered here to be the only ones acting on the system. The development of a general expression allows the inclusion at any time of other forces, such as, for example, the thrust from station-keeping thrusters which are studied in Part II of this paper.

II: A STUDY OF ONE METHOD OF ORBIT ADJUST AND STATION KEEPING

SATELLITE ORBIT AND PARAMETERS

A medium altitude (approximately 6000 nautical miles) satellite orbit was chosen for the included study. The satellite parameters shown in Table 1 are typical for this orbit.* In Part I of this paper a model for the restoring torque, M_{SD} , between the main body and the damper rod was not given. For this study this torque is assumed to be:

$$M_{SD} = C_1 \dot{\rho}_2 + C_2 \rho_2 \quad (25)$$

C_1 is a linear viscous damping coefficient and C_2 is a linear spring coefficient. It is noted that Equation 25 is included in the digital program of Appendix D.

Table 1
Orbit and Satellite Parameters.

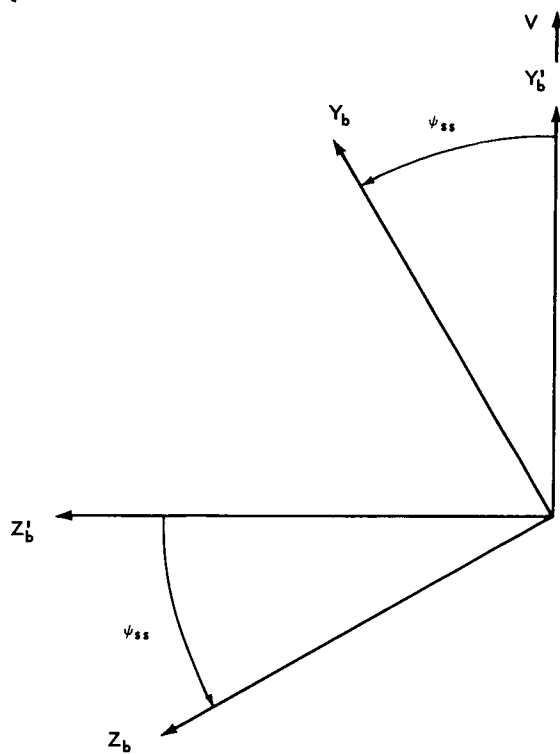
Orbital Period	= 6.4 hours
Satellite Weight	= 600 pounds
I_{xx}	= 394.5 slug-ft ²
I_{yy}	= 3683.0 slug-ft ²
I_{zz}	= 3288.5 slug-ft ²
I_ℓ	= 263.1 slug-ft ²
ρ_1	= 1.0929 radians
ρ_s	= ± 1.0 radians
C_1	= 1.5455 slug-ft ² /sec
C_2	= 4.538 slug-ft ² /sec ²

STEADY STATE DYNAMICS OF THE SATELLITE

The attitude in which the satellite traverses a circular orbit is shown in Figure 7. This motion can best be described as crabbing. The plane of the X , the $X_b - Y_b$ plane, makes an angle of $\psi_{ss} = -20.76$ degrees with the plane of the orbit. The transformation from the body reference system to the prime system, included in Figure 7, will be required later. The primed system is rigidly attached to the satellite body.

Attitude librations are induced by eccentricity in the satellite orbit. The amplitudes of these librations as a function of eccentricity are shown in Figure 8. The in-plane and cross-plane librations correspond to the angles α and ϕ respectively. The orbit period for each of the data points is 6.4 hours. It is noted that for eccentricities of less than 0.05, the increase of in-plane amplitude is nearly linear while the cross-plane libration, though initially smaller, is increasing at a faster rate.

*These data were obtained in a private communication with Mr. H. W. Price of the Stabilization and Control Branch at the Goddard Space Flight Center in Greenbelt, Maryland.



$$\begin{pmatrix} i_b \\ j_b \\ k_b \end{pmatrix} = \begin{pmatrix} 1 & 0 & 0 \\ 0 & \cos \psi_{ss} & \sin \psi_{ss} \\ 0 & -\sin \psi_{ss} & \cos \psi_{ss} \end{pmatrix} \begin{pmatrix} i'_b \\ j'_b \\ k'_b \end{pmatrix}$$

Figure 7—The satellite attitude in a circular orbit transformation from the body reference frame to a body frame in the orbit plane.

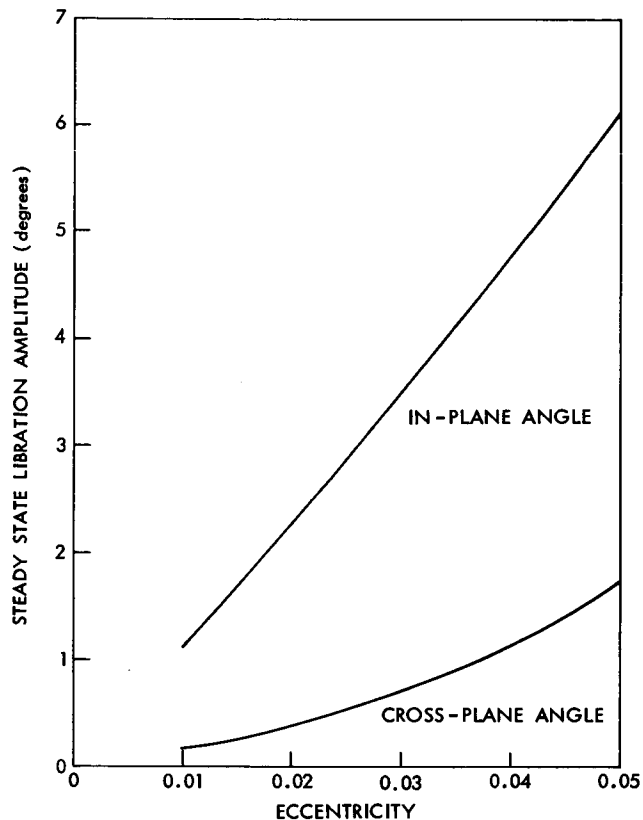


Figure 8—Steady state libration as a function of eccentricity.

SATELLITE RESPONSE TO AN IMPULSIVE TORQUE

Shown in Figure 9 is the response of the satellite to an impulsive torque of 1.3 lb-ft-sec. The impulsive torque was applied in the pitch plane and the satellite orbit was circular. It is seen that the resulting libration amplitude in pitch is reduced to approximately 10% of its initial value in 25 hours time. Note that the yaw angle has turned through 180° and is beginning to stabilize near

$$\psi_{ss} = -20.76 - 180.0 = -200.76^\circ.$$

This second steady-state yaw angle is possible because of the symmetry of the satellite with respect to its X_b - axis.

THRUST PROGRAM

A set of constraints had to be defined before undertaking an orbit adjust and station keeping study. In order to take advantage of having one side of the satellite always facing the earth, an

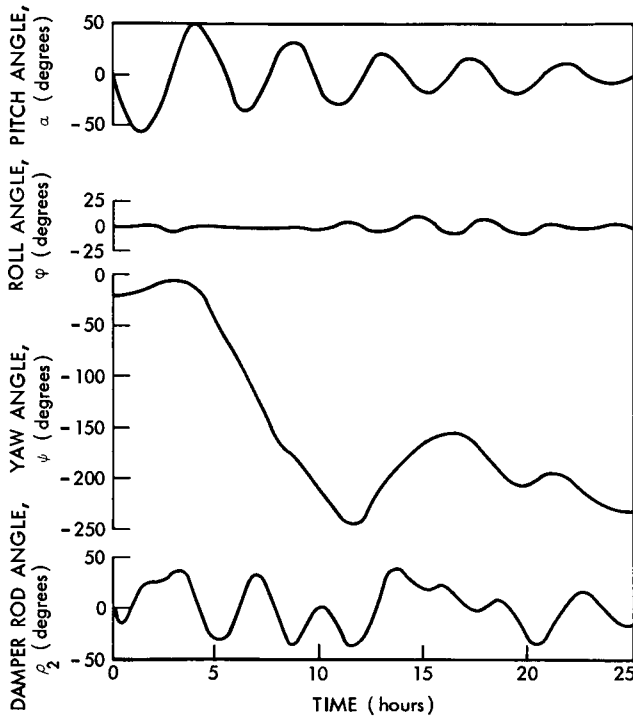


Figure 9—Response of the satellite to an impulsive torque of 1.3 lb-ft-sec.

inversion or turning of the earth pointing axis, x_b , through 180 degrees must be avoided. The determination of a thrust program (thruster on-time per pulse and time between pulses) required to change the orbit eccentricity by 0.01 seemed to be a desirable objective. Parameters to be optimized should be the minimization of the total time required to adjust the eccentricity by the desired amount and minimization of the total fuel expenditure. Additionally, it would be desirable to obtain a thrust program which could be preprogrammed and thus eliminate the necessity of ground monitoring for successful operation.

Two one-pound thrusters placed diametrically opposite each other in direction and with respect to the center of mass of the satellite were selected for this study.* Each of these thrusters was assumed to be 1.5 feet from the center of mass. The possibility of either tangential or radial thrusting being optimum for the above conditions was anticipated, and

individual studies of each were to be made. For the case of tangential thrusting, one of the thrusters was placed on the positive y_b axis and the other on the negative y_b axis (see Figure 7). For the case of radial thrusting, one of the thrusters was placed on the positive x_b axis and the other on the negative x_b axis.

The orientation of the thrust vectors, including thrust misalignment, for tangential and radial thrusting is shown in Figures 10(a) and 10(b), respectively, with respect to the prime body reference frame of Figure 7. The angles δ_1 and δ_2 are defined to give positive components of thrust along the positive x_b and z_b axes when the angles themselves are positive. For this study a total misalignment angle of one degree is assumed. In other words, the magnitudes of δ_1 and δ_2 will be such as to combine into a single solid angle of one degree between the thrust vector and the reference axis. Combining the definitions of δ_1 and δ_2 with the transformation of Figure 7 gives the forces and moments for tangential thrusting to be:

$$F_{x_b} = T \sin \delta_1 \cos \delta_2 ,$$

*The results of this study can be extrapolated to thrust levels other than one pound if the duration of each pulse is small and the time between pulses is the same magnitude when compared to the orbital period; i.e., two pounds of thrust applied for twenty seconds every 3.2 hours produces approximately the same results as does one pound of thrust applied for forty seconds every 3.2 hours.

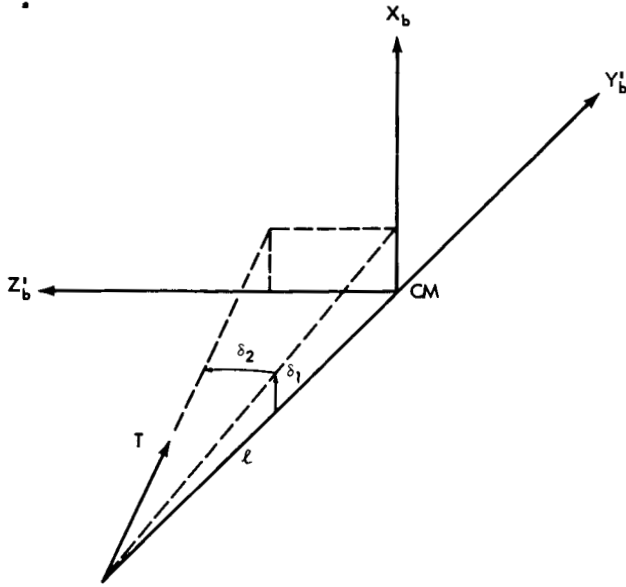


Figure 10a—Orientation of tangential thruster.

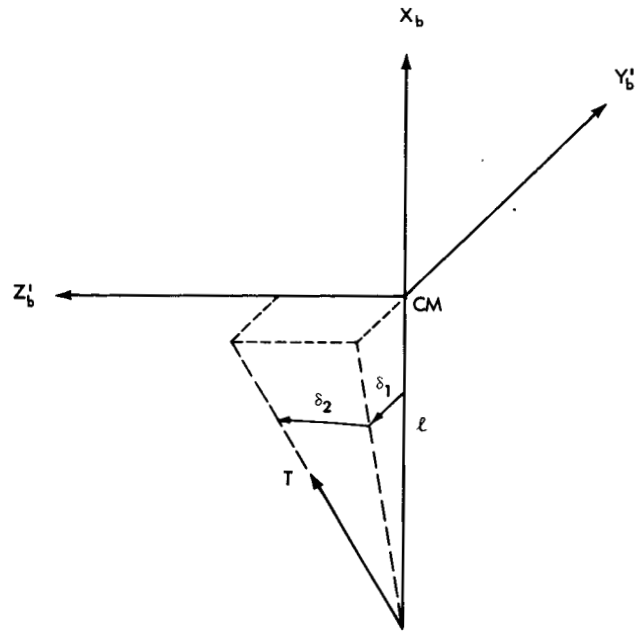


Figure 10b—Orientation of radial thruster.

$$F_{z_b} = T(-\cos \delta_1 \cos \delta_2 \sin \psi_{ss} + \sin \delta_2 \cos \psi_{ss}) , \quad (26)$$

$$M_{x_b} = -Tl \sin \delta_2 ,$$

$$M_{y_b} = Tl \sin \delta_1 \cos \delta_2 \sin \psi_{ss} ,$$

and

$$M_{z_b} = Tl \sin \delta_1 \cos \delta_2 \cos \psi_{ss} ,$$

and for radial thrusting to be:

$$F_{x_b} = T \cos \delta_1 \cos \delta_2 ,$$

$$F_{y_b} = T(-\sin \delta_1 \cos \delta_2 \cos \psi_{ss} + \sin \delta_2 \sin \psi_{ss}) ,$$

$$F_{z_b} = T(\sin \delta_1 \cos \delta_2 \sin \psi_{ss} + \sin \delta_2 \cos \psi_{ss}) , \quad (27)$$

$$M_{x_b} = 0 ,$$

$$M_{y_b} = Tl(\sin \delta_2 \cos \psi_{ss} + \sin \delta_1 \cos \delta_2 \sin \psi_{ss}) ,$$

and

$$M_{z_b} = Tl(-\sin \delta_2 \sin \psi_{ss} + \sin \delta_1 \cos \delta_2 \cos \psi_{ss}) .$$

It is noted that the above Equations 26 and 27 are derived for thrusters located on the negative Y_b and X_b axes, respectively. For sake of simplicity these same equations are assumed for the thrusters on the positive Y_b and X_b axes, and a negative value, $T = -1$ pound, is assigned to thrust magnitude. Although not shown with the basic digital program in Appendix D, the required modification to the program is quite simple. The forces should be evaluated in their body reference frame and then transformed to the geocentric coordinate frame. Program locations A(100) through A(102) have been reserved for this purpose. The moments should be evaluated in their body reference frame and added directly to the program locations A(103) through A(105).

First order perturbation theory provides a method of determining the most opportune times in the orbit for applying thrust pulses to adjust the orbit. To first order the change in eccentricity due to tangential and radial perturbation velocities, which can be attributed in this case to the thrust pulses, are respectively*

$$\frac{de}{dt} = \frac{2 \sqrt{1 - e^2} \cos E}{1 - e \cos E} \frac{\gamma_t}{V},$$

and

(28)

$$\frac{de}{dt} = \sqrt{1 - e^2} \sin E \frac{\gamma_r}{V}.$$

E is the eccentric anomaly, e is the eccentricity, v is the satellite velocity, and γ_t and γ_r are, respectively, tangential and radial perturbation velocities. For small eccentricities, it is seen that tangential pulses should be applied at or near apogee or perigee, and that radial pulses should be applied at approximately ± 90 degrees from apogee or perigee. Thus for the satellite under consideration, the time between pulses should be one-half the orbital period which is 3.2 hours. It is seen also that, all other things being equal, the rate of change of eccentricity for tangential thrusting is approximately twice that for radial thrusting.

The one thing remaining in the definition of the problem is to determine the logic required to know which of the two thrusters to fire. Since no constraint has been placed on the yaw angle, variation between 0 and 360 degrees must be considered for the case of tangential thrusting. Table 2 shows the logic required for tangential thrusting to increase eccentricity. The logic required for radial thrusting is relatively simple, as the problem was constrained to avoid satellite inversion. If the true anomaly of the satellite is between 0 and 180 degrees, the thruster on the negative X_b axis should be fired, and if the true anomaly is between 180 and 360 degrees, the thruster on the positive X_b axis should be fired.

*A geometrical discussion of the effects of tangential and radial perturbations is given in Chapter IX of F. R. Moulton's "Celestial Mechanics", published by The MacMillan Company in 1914. Following similar reasoning, Professor G. D. Bohlor of the Catholic University of America has derived Equations 28 in his unpublished lecture notes for Celestial Mechanics.

Table 2

Logic Required for Tangential Thrusting to Increase Eccentricity. ψ is the Satellite Yaw Angle and θ is the True Anomaly of the Satellite. The Column Under "Thruster" Indicates Whether the Thruster on the Positive Y_b Axis or the One on the Negative Y_b Axis Should be Fired.

ψ (degrees)	θ (degrees)	Thruster
$-110.76 < \psi < +69.24$	$-90 < \theta < +90$	+
$-110.76 < \psi < +69.24$	$+90 < \theta < +270$	-
$+69.24 < \psi < +249.24$	$-90 < \theta < +90$	-
$+69.24 < \psi < +249.24$	$+90 < \theta < +270$	+

DISCUSSION OF RESULTS

Shown in Figure 11 are results of the orbit adjust and station keeping study. The lower half of the graph shows the eccentricity change as a function of time between pulses, with thruster on-time per pulse as parameter. The eccentricity changes are average values based on results from a number of computer runs made for the thrust program indicated, but with the one degree misalignment angle varying around the reference axis (see Figures 10(a) and 10(b)). The points are plotted at multiples of 3.2 hours, which is one-half the initial orbit period. The circled data points indicate tangential thrusting and those points enclosed in diamonds indicate radial thrusting. The protruding arrows show the points which represent a series of runs resulting in at least one satellite inversion. Examination of the circled points without arrows reveals that a 0.01 eccentricity change can be effected in approximately 40 days with either 30-second pulses every 16.0 hours, or 40-second pulses every 22.4 hours. The upper graph of Figure 11 shows that the latter should be chosen as less total impulse and, therefore, less fuel is required. Total impulse is calculated by simply multiplying the thrust level by the total on-time. Also shown on the lower graph of Figure 11 are two points for radial pulses every 22.4 hours. As can be seen, 40-second pulses would produce an eccentricity change of 0.0057 in 40 days. This latter result was suggested by Equations 28,

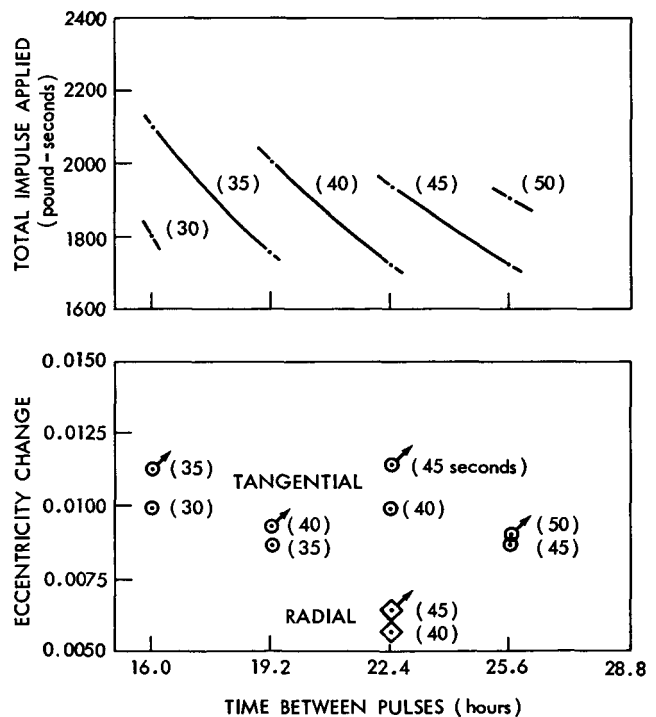


Figure 11—Eccentricity change and total impulse applied versus time between pulses. Thruster on-time per pulse is shown in parenthesis. The total correction time is 40 days.

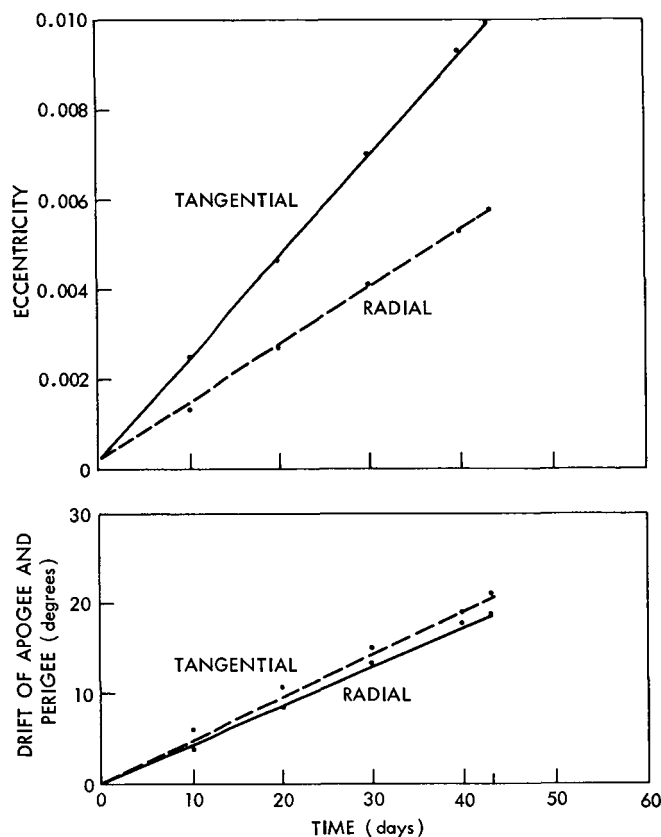


Figure 12—Eccentricity and drift of apogee and perigee for 40-second pulses every 22.4 hours.

after a 0.01 eccentricity change was effected with tangential pulses.

It is significant that both of the tangential data points giving almost a 0.01 eccentricity change in 40 days were pulsed at odd multiples of one-half the orbital period of 3.2 hours. The first multiple was 5 giving 16.0 hours between pulses, and the second was 7 giving 22.4 hours between pulses. This gives pulses alternating between apogee and perigee, which apparently has a self-correcting tendency that pulsing always at either apogee or perigee does not have, as indicated by the lower data points for 18.2 and 25.6 hours between pulses (see Figure 11).

Shown in Figure 12 are the increase in eccentricity and the drift of the satellite from apogee and perigee as a function of time for the 40-second pulses every 22.4 hours. Here the significance is the fact that although the drift has increased to approximately 20 degrees, the eccentricity is still increasing linearly. This means that at least 40 days of preprogrammed thrusting can be planned with no penalty being paid for drift of apogee and perigee.

One desirable objective for the tangential thrusting program was not achieved. Namely, this investigator did not succeed in finding a method of predicting the yaw angle of the spacecraft at the time of the next pulse. (See Table 2 for the yaw angle requirements.) No particular pattern seemed to exist in the data. This means that ground monitoring or some other method of sensing the yaw angle should be provided for tangential thrusting.

Shown in Table 3 are other pertinent data for the series of computer runs representing 40-second pulses every 22.4 hours. It is seen that the number of collisions between the damper rod and its stops is quite high for some misalignment angles when pulsing tangentially, while there are practically no collisions for radial pulsing. The maximum attitude excursions and the maximum attitude angles at the time of impulse are also given. These values seem reasonable.

CONCLUSIONS

The results of this study have shown that for the satellite configuration chosen, a thrust program consisting of 40-second pulses every 22.4 hours minimizes the time required to make a 0.01

Table 3

A Summary of the Results of Orbit Correction for Tangential and Radial Thrusting Using 40-second Pulses Every 22.4 Hours. The Maximum Values are Maximums for the Entire 40 Day Correction Period.

δ_1 (Degrees)	δ_2 (Degrees)	Maximum α (Degrees)	Maximum ϕ (Degrees)	Average Number of Damper Rod Collisions Per Pulse	Maximum Collision Rate of Damper Rod (Radians/ Second)	Maximum α At Time Of Impulse (Degrees)	Maximum ϕ At Time Of Impulse (Degrees)
<u>Tangential Pulses</u>							
0	1.0	17.31	30.47	1.97	0.729×10^{-3}	5.35	8.88
-0.4	0.9	31.32	43.48	1.62	1.018×10^{-3}	14.61	18.09
-0.6	0.8	40.66	45.11	1.60	0.821×10^{-3}	27.95	12.07
-0.7	0.7	40.33	42.30	0.85	0.941×10^{-3}	11.67	13.80
-0.8	0.6	32.75	23.41	0.05	0.496×10^{-3}	3.11	2.41
-0.9	0.4	66.90	46.38	0.45	0.523×10^{-3}	18.73	13.68
-1.0	0	53.74	33.05	0	---	10.17	12.06
<u>Radial Pulses</u>							
0	1.0	36.44	37.61	0	---	5.89	12.29
-0.4	0.9	56.41	51.17	0.03	0.181×10^{-3}	23.24	17.81
-0.6	0.8	42.16	39.28	0	---	9.16	13.95
-0.7	0.7	40.09	41.71	0	---	6.57	15.14
-0.8	0.6	46.23	42.87	0	---	8.05	9.47
-0.9	0.4	44.18	26.29	0	---	8.72	7.95
-1.0	0	55.36	36.12	0.02	0.099×10^{-3}	9.83	6.93

eccentricity change in the orbit and minimizes the fuel required. A one pound thrust level and a one degree thruster misalignment angle were assumed for the study. If tangential thrusting is used, the 0.01 eccentricity change can be effected in 40 days. However, a means of sensing the yaw angle of the satellite must be provided in order to establish the direction in which successive pulses should be made. Additionally, tangential thrusting results in a significant number of collisions between the damper rod and its mechanical stops. No attempt was made to evaluate these collisions and rates of collision in terms of material strengths.

Should sensing the yaw angle and the damper rod collisions prove to be unsatisfactory, radial thrusting can be used. Both of the problems, sensing the yaw angle and the rod collisions, are avoided, but at the expense of almost doubling the time required to adjust the orbit. In 40 days, radial thrusting produces an eccentricity change of only 0.0057.

(Manuscript received February 9, 1966)

REFERENCES

1. Roberson, R. E., "Attitude Control of Satellites and Space Vehicles," in: *Advances in Space Sciences*, Vol. 2, New York: Academic Press, Inc., 1960, pp. 351-436.

2. Paul, B., "Planar Librations of an Extensible Dumbbell Satellite," *Amer. Inst. Aeronaut. and Astronaut. Jour.*, 1(2):411-418, February 1963.
3. Fischell, R. E., "The TRAAC Satellite," *Appl. Phys. Lab. Tech. Dig.*, 1(3):3-9, Jan. - Feb. 1962.
4. Kamm, L. J., "Vertistat: An Improved Satellite Orientation Device," *Am. Rocket Soc. Jour.*, 32(6):911-913, June 1962.
5. Tinling, B. E., and Merrick, V. K., "The Exploitation of Inertial Coupling in Passive Gravity-Gradient Stabilized Satellites," *Amer. Inst. Aeronaut. and Astronaut.*, Paper 63-342(A63-21599), August 12, 1963; also in: *Jour. of Spacecraft and Rockets*, 1(4):381-387, July-August 1964.
6. Constant, F. W., "Theoretical Physics," London: Addison-Wesley Pub. Co., Inc., 1954, pp. 71 and 152.
7. Jenson, J., Kraft, J. D., and Townsend, B. E., Jr., "Orbital Mechanics," in: *Orbital Flight Handbook, Vol. 1; Part 1: Basic Techniques and Data*, NASA Special Publication SP-33, Washington: National Aeronautics and Space Administration, March 1963, pp. III-1 to III-41.
8. Roberson, R. E., and Tatistcheff, D., "The Potential Energy of a Small Rigid Body in the Gravitational Field of an Oblate Spheroid," *J. Franklin Inst.*, 262(9):209-214, September 1956.
9. Roberson, R. E., "Gravitational Torque on a Satellite Vehicle," *J. Franklin Inst.*, 265(1):13-22, January 1958.
10. DeBra, D. B., "Vectors and Dyadics: The Natural Tools of Space Vehicle Mechanics," in: *Advances in Astronautical Sciences*, Vol. 9:77-107, Proc. of 4th Western Regional Meeting of the American Astronautical Society, San Francisco, 1-3 August 1961; New York: AA5, 1963.

Appendix A

List of Symbols

\vec{A}	acceleration vector of satellite center of mass
A	azimuth angle
C_1	linear viscous damping coefficient
C_2	linear spring coefficient
\vec{F}	external forces acting on the satellite
E	eccentric anomaly of the satellite
e	eccentricity of the satellite orbit
\vec{H}	total angular momentum of the satellite main body
\vec{H}_T	total angular momentum of both the main body and the damper rod
I	moment of inertia tensor of satellite main body
$\{i, j, k\}$	unit vectors along coordinate axes X, Y, Z
J	total moment of inertia tensor including damper rod contribution
K	inverse of the total moment of inertia tensor
L	the inertia tensor for momentum transfer between the two satellite sections at the time of collision
\vec{M}	gravitational moment exerted on the satellite by the earth
M_{SD}	restoring torque exerted on the rod by the spring-damper mechanism
m	mass
\vec{R}	reaction torque between the two satellite sections
$\{r, \Lambda, \phi_c\}$	inertial spherical coordinates of the satellite
T	thrust magnitude of orbit adjust thrusters
$\begin{pmatrix} T \\ \lambda \rightarrow \beta \end{pmatrix}$	matrix defining vector transformation from λ -base coordinate system to β -base system
\vec{V}	inertial velocity vector of the satellite center of mass
$\{X, Y, Z\}$	orthogonal right-handed coordinate axes
$\{\alpha, \phi, \psi\}$	pitch, roll, yaw angles of satellite measured from attitude reference system

ψ_{ss}	steady state yaw angle
Δ	determinant of the total moment of inertia tensor
$\{\delta_1, \delta_2\}$	thrust misalignment angles
$\{\gamma_t, \gamma_r\}$	tangential and radial perturbation velocities
ζ	total external moments acting on the satellite
μ	earth gravitational constant
$\vec{\Omega}$	inertial angular velocity vector of the satellite
ρ_1	dihedral angle between rod rotation plane and satellite x plane
ρ_2	angular deviation of damper rod from equilibrium position
$\pm\rho_s$	maximum allowable deviation angles made by rod before hitting stops
θ	true anomaly of the satellite

Subscripts

b	refers to main body coordinate system
c	refers to geocentric coordinate system
d	refers to damper rod coordinate system
o	refers to attitude reference or orbital coordinate system
ℓ	refers to the length of the damper rod
r	refers to the radius of the damper rod
$\{r, \Lambda, \phi_c\}$	refers to inertial spherical coordinates of the satellite
$\{x, y, z\}$	refers to a specified coordinate system

Appendix B

Elements Defining a Satellite Orbit

The orbit of a satellite around the earth is, according to Kepler's first law, an ellipse with the earth located at one focus. The semimajor axis (a) and the eccentricity (e) define the size and shape of the ellipse, while the parameter (τ) denotes the time of perigee passage of the satellite. These three elements permit calculation of the vehicle position in its orbit plane at any time.

An additional set of three variables is also required to orient the orbit plane itself. As shown in Figure B1, the longitude of the ascending node ($\bar{\Omega}$) determines the line of intersection of the orbital plane and the earth's equatorial plane, the element (I) specifies the angle at which the orbital plane is inclined to the equator, and the longitude of perigee ($\bar{\omega} + \theta$) determines the direction of perigee with respect to the vernal equinox. The six elements a , e , τ , $\bar{\Omega}$, I , and ($\bar{\omega} + \theta$) are called orbital elements, and all six are required to completely specify the satellite orbit in relation to the earth.

These elements designate position as a function of time, and therefore implicitly contain the satellite velocity components. The solution of the translational equations of motion (Equation 3) requires velocity-dependent and position-dependent terms as initial conditions, but referred to the inertial coordinate system. Conversion from orbital elements to inertial elements may be effected as follows:

(1) Position elements r , ϕ_c , Λ :

For r ,

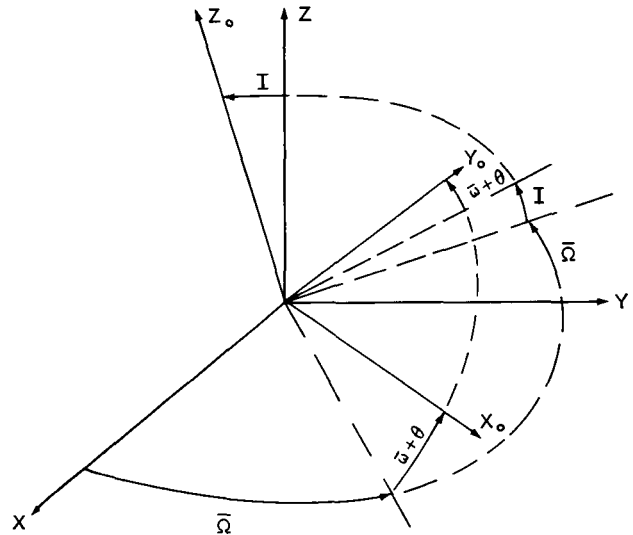
$$r = \frac{a(1 - e^2)}{1 + e \cos \theta} \quad (\text{B1})$$

(θ = true anomaly; determined from e and τ);

for ϕ_c ,

$$\sin \phi_c = \sin I \sin (\bar{\omega} + \theta), \quad (\text{B2-a})$$

$$\cos \phi_c \geq 0; \quad (\text{B2-b})$$



$$\begin{pmatrix} i \\ j \\ k \end{pmatrix} = \begin{pmatrix} -\sin \bar{\Omega} \cos I \sin (\bar{\omega} + \theta) & -\sin \bar{\Omega} \cos I \cos (\bar{\omega} + \theta) & \sin \bar{\Omega} \sin I \\ +\cos \bar{\Omega} \cos (\bar{\omega} + \theta) & -\cos \bar{\Omega} \sin (\bar{\omega} + \theta) & \\ \cos \bar{\Omega} \cos I \sin (\bar{\omega} + \theta) & \cos \bar{\Omega} \cos I \cos (\bar{\omega} + \theta) & -\cos \bar{\Omega} \sin I \\ +\sin \bar{\Omega} \cos (\bar{\omega} + \theta) & -\sin \bar{\Omega} \sin (\bar{\omega} + \theta) & \\ \sin I \sin (\bar{\omega} + \theta) & \sin I \cos (\bar{\omega} + \theta) & \cos I \end{pmatrix} \begin{pmatrix} i_0 \\ j_0 \\ k_0 \end{pmatrix}$$

Figure B1—Rotational transformation from the orbit or attitude to the inertial reference frame.

for Λ ,

$$\sin \Lambda = \frac{1}{\cos \phi_c} \left[\cos \bar{\Omega} \cos I \sin (\bar{\omega} + \theta) + \sin \bar{\Omega} \cos (\bar{\omega} + \theta) \right], \quad (\text{B3-a})$$

$$\cos \Lambda = \frac{1}{\cos \phi_c} \left[\cos \bar{\Omega} \cos (\bar{\omega} + \theta) - \sin \bar{\Omega} \cos I \sin (\bar{\omega} + \theta) \right]. \quad (\text{B3-b})$$

(2) Velocity elements \dot{r} , $r^2 \dot{\phi}_c$, $r^2 \dot{\Lambda} \cos^2 \phi_c$:

For \dot{r} ,

$$\dot{r} = \sqrt{\frac{\mu}{a(1-e^2)}} e \sin \theta \quad (\text{B4})$$

(Reference 7, p.III-22). The two remaining terms arise in the following manner: Noting that from Figure 4b:

$$\dot{\Lambda} \cos \phi_c = \xi_{z_0} \cos A, \quad (\text{B5-a})$$

$$\dot{\phi}_c = \xi_{z_0} \sin A, \quad (\text{B5-b})$$

and from Reference 7, p. III-23,

$$\dot{\theta} = \xi_{z_0} = \sqrt{\frac{\mu}{a^3(1-e^2)^3}} (1+e \cos \theta)^2 = \sqrt{\frac{\mu(1+e \cos \theta)}{r^3}}. \quad (\text{B6})$$

Solution for the two remaining constants by substitution yields, for $r^2 \dot{\phi}_c$:

$$r^2 \dot{\phi}_c = \sqrt{\mu r(1+e \cos \theta)} \sin A, \quad (\text{B7})$$

for $r^2 \dot{\Lambda} \cos^2 \phi_c$:

$$r^2 \dot{\Lambda} \cos^2 \phi_c = \sqrt{\mu r(1+e \cos \theta)} \cos \phi_c \cos A. \quad (\text{B8})$$

After internal calculations have been completed in inertial coordinates, conversion to orbital elements may be done through the following equations:

For I:

$$\cos I = \cos \phi_c \cos A,$$

$$\sin I \geq 0; \quad (\text{B9})$$

For $\bar{\Omega}$:

$$\begin{aligned}\sin \bar{\Omega} &= (\sin \Lambda \sin A - \cos \Lambda \sin \phi_c \cos A) / \sin I, \\ \cos \bar{\Omega} &= (\cos \Lambda \sin A + \sin \Lambda \sin \phi_c \cos A) / \sin I ;\end{aligned}\tag{B10}$$

For $(\bar{\omega} + \theta)$:

$$\begin{aligned}\sin (\bar{\omega} + \theta) &= \sin \phi_c / \sin I, \\ \cos (\bar{\omega} + \theta) &= (\cos \phi_c \sin A) / \sin I.\end{aligned}\tag{B11}$$

When the orbit plane coincides with the earth equatorial plane ($I = 0$), then $\phi_c = A = 0$. By defining the longitude of ascending node ($\bar{\Omega}$) to be zero, it follows that

$$\bar{\omega} + \theta = \Lambda.\tag{B12}$$

Defining the element $Q = rv^2/\mu$ and $\cos^2 \Gamma = v_A^2 - v_{\phi_c}^2 / v^2$, the determination of elements (a) and (e) are:

$$a = \frac{r}{2-Q},\tag{B13}$$

and

$$e = \sqrt{1 - Q(2-Q) \cos^2 \Gamma}\tag{B14}$$

If the orbit is not circular ($e \neq 0$), it may be shown that

$$\theta = \tan^{-1} \left[\frac{v_r}{\sqrt{v_A^2 + v_{\phi_c}^2} - \sqrt{\frac{\mu}{a(1-e^2)}} \right].\tag{B15}$$

If the orbit is circular, define $\bar{\omega} = 0$.

Appendix C

Gravitational Moments Generated by Earth Potential

Roberson (References 8 and 9) has shown the rotational potential of a satellite vehicle under the influence of a μ/r^2 gravity force field to be

$$U = \frac{3\mu I_0}{2r^3}, \quad (C1)$$

where I_0 is the instantaneous moment of inertia of the satellite about the local geocentric vertical. When expressed in terms of the body moments of inertia and the attitude deviation angles α , ϕ , and ψ , the result is

$$I_0 = I_{xx}a_1^2 + I_{yy}a_2^2 + I_{zz}a_3^2 + 2I_{xy}a_1a_2 + 2I_{xz}a_1a_3 + 2I_{yz}a_2a_3, \quad (C2)$$

where

$$a_1 = \cos \alpha \cos \phi,$$

$$a_2 = -\cos \alpha \sin \phi \sin \psi - \sin \alpha \cos \psi,$$

and

$$a_3 = -\cos \alpha \sin \phi \cos \psi + \sin \alpha \sin \psi.$$

DeBra (Reference 10) points out that work is related to a change in potential by

$$\vec{M} \cdot d\alpha_\tau = -dU, \quad (C3)$$

where \vec{M} = total moment, and

$$d\alpha_\tau = \text{resultant of incremental changes in } d\alpha, d\phi, \text{ and } d\psi.$$

Expressing the elements $d\alpha$, $d\phi$, $d\psi$ in body coordinates gives

$$\vec{M}_b \cdot B \cdot d\alpha_\tau = - \left[\frac{\partial U}{\partial \alpha}, \frac{\partial U}{\partial \phi}, \frac{\partial U}{\partial \psi} \right] \cdot d\alpha_\tau, \quad (C4)$$

or

$$\vec{M}_b \cdot B = - \left[\frac{\partial U}{\partial \alpha}, \frac{\partial U}{\partial \phi}, \frac{\partial U}{\partial \psi} \right],$$

where \vec{M}_b denotes the total moment, now referred to body coordinates; and the dyadic B is given by the matrix,

$$B = \begin{pmatrix} \sin \phi & 0 & 1 \\ \cos \phi \sin \psi & -\cos \psi & 0 \\ \cos \phi \cos \psi & \sin \psi & 0 \end{pmatrix} \quad (C5)$$

It follows from Equation C-4 that

$$\begin{pmatrix} M_{x_b} \\ M_{y_b} \\ M_{z_b} \end{pmatrix} = - \begin{pmatrix} \\ \\ \\ \end{pmatrix}^t B^{-1} \begin{pmatrix} \frac{\partial U}{\partial \alpha} \\ \frac{\partial U}{\partial \phi} \\ \frac{\partial U}{\partial \psi} \end{pmatrix}, \quad (C6)$$

or

$$\begin{aligned} M_{x_b} &= - \frac{\partial U}{\partial \psi}, \\ M_{y_b} &= - \frac{\partial U}{\partial \alpha} \frac{\sin \psi}{\cos \phi} + \frac{\partial U}{\partial \phi} \cos \psi + \frac{\partial U}{\partial \psi} \frac{\sin \phi \sin \psi}{\cos \phi}, \\ M_{z_b} &= - \frac{\partial U}{\partial \alpha} \frac{\cos \psi}{\cos \phi} - \frac{\partial U}{\partial \phi} \sin \psi + \frac{\partial U}{\partial \psi} \frac{\sin \phi \cos \psi}{\cos \phi}, \end{aligned} \quad (C7)$$

which gives the expressions

$$\begin{aligned} M_{x_b} &= \frac{-3\mu}{r^3} \left[(I_{yy} - I_{zz}) a_2 a_3 + I_{xy} a_1 a_3 - I_{xz} a_1 a_2 + I_{yz} (a_3^2 - a_2^2) \right], \\ M_{y_b} &= \frac{-3\mu}{r^3} \left[(I_{zz} - I_{xx}) a_1 a_3 - I_{xy} a_2 a_3 + I_{xz} (a_1^2 - a_3^2) + I_{yz} a_1 a_2 \right], \\ M_{z_b} &= \frac{-3\mu}{r^3} \left[(I_{xx} - I_{yy}) a_1 a_2 + I_{xy} (a_2^2 - a_1^2) + I_{xz} a_2 a_3 - I_{yz} a_1 a_3 \right]. \end{aligned} \quad (C8)$$

The moment referred to the rod coordinates may be calculated by noting that

$$\begin{pmatrix} i_d \\ j_d \\ k_d \end{pmatrix} = \begin{pmatrix} T \\ b \rightarrow d \end{pmatrix} \begin{pmatrix} i_b \\ j_b \\ k_b \end{pmatrix}, \quad \begin{pmatrix} T \\ b \rightarrow d \end{pmatrix} = \begin{pmatrix} T \\ d \rightarrow b \end{pmatrix}^{-1}$$

The moment terms, when referred to this system, are given by

$$M_{x_d} = 0,$$

$$M_{y_d} = \frac{-3\mu}{r^3} I_l b_1 b_3, \quad (C9)$$

$$M_{z_d} = \frac{3\mu}{r^3} I_l b_1 b_2,$$

where

$$b_1 = a_1 \sin \rho_2 + a_2 \cos \rho_2 \cos \rho_1 + a_3 \cos \rho_2 \sin \rho_1,$$

$$b_2 = -a_2 \sin \rho_1 + a_3 \cos \rho_1,$$

$$b_3 = a_1 \cos \rho_2 - a_2 \sin \rho_2 \cos \rho_1 - a_3 \sin \rho_2 \sin \rho_1.$$

Appendix D

A Gravity-Oriented Satellite Digital Program

INTRODUCTION

The motion of a two-body, gravity-oriented satellite has been implicitly determined by a set of seven second-order differential equations. Three of these equations locate the satellite in an inertial reference system, three specify its attitude with respect to a designated attitude reference system, and the seventh describes the motion of the damper rod in relation to the main body.

A numerical technique which facilitates obtaining useful results is now presented. The program, developed along lines similar to a program by Dennison and Butler*, is written in FORTRAN II format and occupies approximately 7000 words of memory on the SDS-920 computer. This includes all necessary standard library subroutines, as well as the main program and attendant subroutines.

A listing of the input variables, to determine the initial conditions of the equations, and vehicle parameters is included. From these the single-step Runge-Kutta quadrature program generates successive values of the orbit location and vehicle attitude angles, along with the rod deviation angle. A choice of output options is provided.

The program as it presently stands includes only gravitational forces and moments generated by the earth on the satellite, but it can be readily adapted to accommodate additional forces and moments from other sources through the addition of an intermediate subroutine. To facilitate this or any other change that might be desired, internal variables are listed and defined, and the program listing (see Table D10) is interlaced with comment statements.

EQUATION LISTING

The previously derived equations defining the satellite motion are described briefly in this section. Reference should be made to the derivation for secondary equations, and to the accompanying list of symbols for definitions.

*Dennison, A. J., and Butler, J. F., "Missile and Satellite Systems Program for the IBM-7090", Technical Report 61-SD-170 (The General Electric Co., Missile and Space Division, King of Prussia, Pa.), prepared on contract to NASA, unpublished.

Translational Motion

The variables (r, Λ, ϕ_c) are determined by doubly integrating Equation(s) 3, which are repeated here as:

$$\begin{aligned}\ddot{r} &= (r \dot{\Lambda}^2 \cos^2 \phi_c + r \dot{\phi}_c^2) + \frac{F_r}{m}, \\ \frac{d}{dt} (r^2 \dot{\Lambda} \cos^2 \phi_c) &= \frac{F_\Lambda}{m} (r \cos \phi_c), \\ \frac{d}{dt} (r^2 \dot{\phi}_c) &= r \left(\frac{F_{\phi_c}}{m} - r \dot{\Lambda}^2 \sin \phi_c \cos \phi_c \right).\end{aligned}\tag{D1}$$

Rotational Motion

The inertial body rate, $\vec{\Omega}$, is determined by integrating Equation (12), which is repeated here as:

$$\begin{pmatrix} \dot{\Omega}_{x_b} \\ \dot{\Omega}_{y_b} \\ \dot{\Omega}_{z_b} \end{pmatrix} = \frac{1}{\Delta} \begin{pmatrix} K_{xx} & K_{xy} & K_{xz} \\ K_{xy} & K_{yy} & K_{yz} \\ K_{xz} & K_{yz} & K_{zz} \end{pmatrix} \begin{pmatrix} \delta_{x_b} \\ \delta_{y_b} \\ \delta_{z_b} \end{pmatrix}.\tag{D2}$$

The attitude deviation angles are then determined by integrating Equation(s) (20), which are repeated here as:

$$\begin{aligned}\dot{\alpha} &= \frac{1}{\cos \phi} \left[(\Omega_{y_b} - \xi_{y_b}) \sin \psi + (\Omega_{z_b} - \xi_{z_b}) \cos \psi \right], \\ \dot{\phi} &= - (\Omega_{y_b} - \xi_{y_b}) \cos \psi + (\Omega_{z_b} - \xi_{z_b}) \sin \psi, \\ \dot{\psi} &= \Omega_{x_b} - \xi_{x_b} - \dot{\alpha} \sin \phi.\end{aligned}\tag{D3}$$

Rod Motion

The rod motion, defined by the variable ρ_2 , is found by doubly integrating Equation (13), which is repeated here as:

$$\ddot{\rho}_2 = - \dot{\Omega}_{y_b} \sin \rho_1 + \Omega_{z_b} \cos \rho_1 - \Omega_{z_d} \Omega_{x_d} - \frac{1}{I_\ell} (M_{y_d} + M_{SD}).\tag{D4}$$

In Equation (D4), the spring restoring torque M_{SD} is defined by the equation:

$$M_{SD} = C_1 \dot{\rho}_2 + C_2 \rho_2$$

Since ρ_2 is dimensionally a pure numeric, it follows that C_1 has the dimensions

$$[m] [l^2] [t^{-1}] ,$$

and C_2 has the dimensions

$$[m] [l^2] [t^{-2}] .$$

COMPUTER PROGRAM

Flow Chart

The main program and associated subroutines are related, as shown in Figure D1.

Program Description

The *Main Program* [MAIN] performs three major functions prior to calling the integration subroutine: (a) initial read-in and/or computation of all constant vehicle parameters used in the program, values stored in the (A) matrix from A(50) through A(97), (b) read-in of initial conditions for rotational equations of motion and for equation of damped-rod motion, and (c) read-in of orbital elements and conversion to initial conditions in the inertial coordinate system for the translational equations of motion.

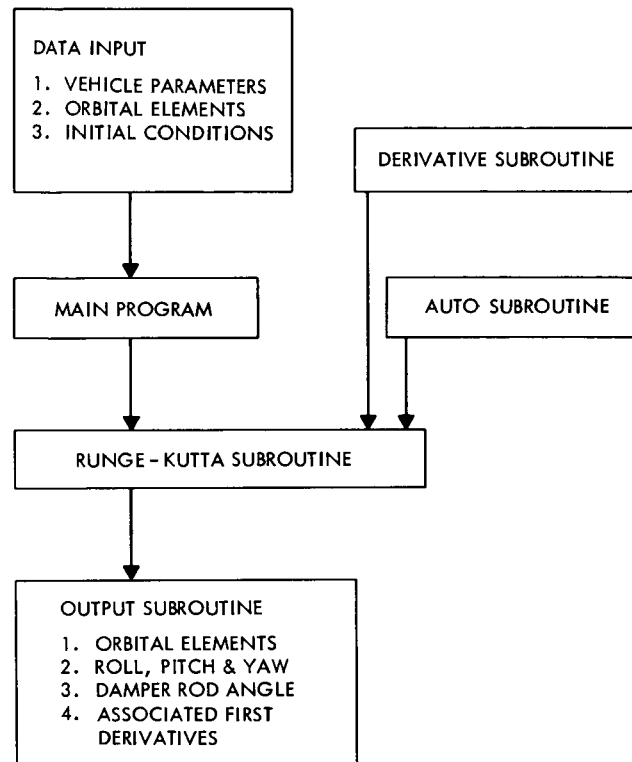


Figure D1—Main program and associated subroutines for numerical determination of the equations of motion of a gravity-gradient satellite. Standard FORTRAN II library subroutines used are arctangent, cosine, sine, and square root.

The *vehicle parameter input format* is listed in Table D1, and is entered into the computer after WRITE OUTPUT TAPE 3, 2 of the main program.

The *input format for initial conditions and orbital elements* is listed in Table D2, and is entered into the computer after A(97) = A(62)**2 of the main program. Following the evaluation of these inputs, control is transferred to the integration subroutine RK(N).

Table D1
Vehicle Parameter Input Format.

ENTRY TAPE	ENTRY CODE	PARAMETER	UNITS OF MEASURE
READ INPUT TAPE 2,1,	A(50)	Vehicle mass	Slugs
	A(51)	Rod mass	Slugs
READ INPUT TAPE 2,1,	A(53)	Vehicle inertia moment (x)	Slug-ft. ²
	A(54)	Vehicle inertia moment (y)	Slug-ft. ²
	A(55)	Vehicle inertia moment (z)	Slug-ft. ²
READ INPUT TAPE 2,1,	A(59)	Vehicle inertia product (xy)	Slug-ft. ²
	A(60)	Vehicle inertia product (xz)	Slug-ft. ²
	A(61)	Vehicle inertia product (yz)	Slug-ft. ²
READ INPUT TAPE 2,1,	A(62)	Rod inertia moment	Slug-ft. ²
	A(63)	Damper plane inclination	Degrees
READ INPUT TAPE 2,1,	A(66)	C ₁	Slug-ft. ² /sec.
	A(67)	C ₂	Slug-ft. ² /sec. ²

Table D2
Input Format for Initial Conditions and Orbital Elements.

ENTRY TAPE	ENTRY CODE	PARAMETER	UNITS OF MEASURE
READ INPUT TAPE 2,1,	AA	Semimajor axis	Feet
	ECC	Eccentricity	Numeric
	XI	Orbit Plane Inclination	Degrees
READ INPUT TAPE 2,1,	THE	True Anomaly	Degrees
	AP	Argument of Perigee	Degrees
	AN	Longitude of Ascending Node	Degrees
READ INPUT TAPE 2,1,	Y(7)	Inertial body rate (x)	Rad./sec.
	Y(8)	Inertial body rate (y)	Rad./sec.
	Y(9)	Inertial body rate (z)	Rad./sec.
READ INPUT TAPE 2,1,	Y(10)	Pitch angle	Degrees
	Y(11)	Roll angle	Degrees
	Y(12)	Yaw angle	Degrees
READ INPUT TAPE 2,1,	Y(13)	Rod angular velocity	Rad./sec.
	Y(14)	Damper rod angle	Degrees
READ INPUT TAPE 2,1,	Y(15)	Machine integration time	Seconds
	Y(16)	Integration interval	Seconds
	Y(17)	Printout interval	Seconds
	Y(18)	Termination time	Seconds

The *Runge-Kutta Subroutine* [RK(N)] performs the fourth-order integration procedure. Upon completion of this subroutine function, control is transferred back to the main program, resulting in the termination of the computer program.

Entry into the *Derivative Subroutine* [DERIV] is from subroutine RK(N) for the purpose of computing the values of the differential equations at each successive point for each differential equation. Control is then returned to subroutine RK(N).

Entry into the *Momentum Transfer Subroutine* [AUTO (FLAG, STP)] is from subroutine RK(N), for the purpose of computing momentum transfer when the damper rod collides with the stops mounted on the main vehicle. Time of collision and relative angular velocity between the sections are written on output tape; control is then returned to subroutine RK(N).

The *Data Output Subroutine* [OUT(K)] is called by subroutine RK(N) in order to convert integrated values of the sought-after variables to the proper output format. The translational coordinates are converted to orbital element representation, while all angular measures are converted from radians to degrees. Depending on the value of K (either 0 or 1), one of two possible output modes, described in Table D3, is activated.

Table D3
Data Output Subroutine.

OUTPUT TAPE	CODE	PARAMETER	UNITS
OUTPUT MODE (0)			
WRITE OUTPUT TAPE 3,32, (LINE 30)	THR	Time	Hours
	PITCH	Pitch angle	Degrees
	ROLL	Roll angle	Degrees
	YAW	Yaw angle	Degrees
	RHO2	Damper rod angle	Degrees
OUTPUT MODE (1)			
WRITE OUTPUT TAPE 3,20, WRITE OUTPUT TAPE 3,21,	THR	Time	Hours
	Y(15)	Time	Seconds
	PITCH	Pitch angle	Degrees
	Y(7)	Inertial body rate (x)	Rad./sec.
	AA	Semimajor axis	Feet
WRITE OUTPUT TAPE 3,21,	THE	True anomaly	Degrees
	ROLL	Roll angle	Degrees
	Y(8)	Inertial body rate (y)	Rad./sec.
	ECC	Eccentricity	Numeric
	AP	Argument of perigee	Degrees
WRITE OUTPUT TAPE 3,21,	YAW	Yaw angle	Degrees
	Y(9)	Inertial body rate (Z)	Rad./sec.
	XI	Orbit inclination	Degrees
	AN	Longitude of ascending node	Degrees
	Y(4)	Radius	Feet
WRITE OUTPUT TAPE 3,20	V	Velocity	Ft./sec.
	RHO2	Damper rod angle	Degrees
	Y(13)	Rod angular velocity	Rad./sec.

MATRIX ELEMENTS

Most of the physical quantities computed in the program are assigned to one-dimensional arrays "A" and "Y". This eliminates the necessity of inventing meaningful alphabetic characters to name each of these quantities individually. A less obvious advantage to persons familiar with FORTRAN is the ease with which information can be transferred between subroutines by simply

putting these arrays in "COMMON". It is noted that several of the array elements are intentionally undefined in the present program, to facilitate addition of features such as special thrust routines, higher order gravitational calculations, and a more exact mathematical model of the spring-damper mechanism.

The first fourteen elements of the Y-array have been assigned to the basic variables for the seven-degree-of-freedom equations of motion. The time derivatives of these variables have been assigned to the corresponding A-array elements indicated in Table D4.

Table D4
Elements of Translational and Rotational Motion.

ELEMENT	PARAMETER	ELEMENT	PARAMETER
A(1)	\ddot{r}	Y(1)	\dot{r}
A(2)	$\frac{d}{dt} (r^2 \dot{\Lambda} \cos^2 \phi_c)$	Y(2)	$r^2 \dot{\Lambda} \cos^2 \phi_c$
A(3)	$\frac{d}{dt} (r^2 \dot{\phi}_c)$	Y(3)	$r^2 \dot{\phi}_c$
A(4)	\dot{r}	Y(4)	r
A(5)	$\dot{\Lambda}$	Y(5)	Λ
A(6)	$\dot{\phi}_c$	Y(6)	ϕ_c
A(7)	$\dot{\Omega}_{x_b}$	Y(7)	Ω_{x_b}
A(8)	$\dot{\Omega}_{y_b}$	Y(8)	Ω_{y_b}
A(9)	$\dot{\Omega}_{z_b}$	Y(9)	Ω_{z_b}
A(10)	$\dot{\alpha}$	Y(10)	α
A(11)	$\dot{\phi}$	Y(11)	ϕ
A(12)	$\dot{\psi}$	Y(12)	ψ
A(13)	$\ddot{\rho}_2$	Y(13)	$\dot{\rho}_2$
A(14)	$\dot{\rho}_2$	Y(14)	ρ_2

Integration Control Parameters

The integration control parameters are as follows:

Y(15) = Current machine integration time,

Y(16) = Integration time interval,

Y(17) = Printout time interval,

Y(18) = Termination time.

Satellite Inertial Parameters

The satellite inertial parameters A(50) through A(97) in Table D5 remain constant for any given run. The repeated unnecessary entry into the sine-cosine subroutine and other arithmetic operations required for A(75) through A(97) is avoided by making these calculations early in the program (*Main Program*) and retaining them for later use. The resulting time saved is appreciable.

Table D5
Vehicle Inertia Parameters.

ELEMENT	PARAMETER	ELEMENT	PARAMETER
A(50)	m_b	A(75)	$I_{yy}I_{zz} - I_{yz}^2$
A(51)	m_d	A(76)	$I_{xz}I_{yz} - I_{zz}I_{xy}$
A(52)	$m_b + m_d$	A(77)	$I_{xy}I_{yz} - I_{yy}I_{xz}$
A(53)	I_{xx}	A(78)	$(I_{xx} + I_\ell)I_{zz} - I_{xz}^2$
A(54)	I_{yy}	A(79)	$I_{xy}I_{xz} - (I_{xx} + I_\ell)I_{yz}$
A(55)	I_{zz}	A(80)	$(I_{xx} + I_\ell)I_{yy} - I_{xy}^2$
A(56)	$I_{yy} - I_{zz}$	A(81)	$I_\ell(I_{yy}\sin^2\rho_1 - 2I_{yz}\sin\rho_1\cos\rho_1 + I_{zz}\cos^2\rho_1)$
A(57)	$I_{zz} - I_{xx}$	A(82)	$I_\ell(-I_{yz}\sin\rho_1 + I_{zz}\cos\rho_1)$
A(58)	$I_{xx} - I_{yy}$	A(83)	$I_\ell(-I_{xy}\sin\rho_1 + I_{xz}\cos\rho_1)\sin\rho_1$
A(59)	I_{xy}	A(84)	$I_\ell(I_{yy}\sin\rho_1 - I_{yz}\cos\rho_1)$
A(60)	I_{xz}	A(85)	$I_\ell(I_{xy}\sin\rho_1 - I_{xz}\cos\rho_1)\cos\rho_1$
A(61)	I_{yz}	A(86)	$2I_\ell I_{xz}\sin\rho_1$
A(62)	I_ℓ	A(87)	$I_\ell(I_{xx}\sin^2\rho_1 - I_{zz})$
A(63)	ρ_1	A(88)	$I_\ell(-I_{xx}\sin\rho_1\cos\rho_1 + I_{yz})$
A(64)	$\sin\rho_1$	A(89)	$-I_\ell(I_{xy}\sin\rho_1 + I_{xz}\cos\rho_1)$
A(65)	$\cos\rho_1$	A(90)	$2I_\ell I_{xy}\cos\rho_1$
A(66)	C_1	A(91)	$I_\ell(I_{xx}\cos^2\rho_1 - I_{yy})$
A(67)	C_2	A(92)	$I_\ell(I_{yy}\cos^2\rho_1 + 2I_{yz}\sin\rho_1\cos\rho_1 + I_{zz}\sin^2\rho_1)$
A(68)	$I_{xx} + I_\ell$	A(93)	$-I_\ell(I_{xy}\cos\rho_1 + I_{xz}\sin\rho_1)$
A(69)	$\sin^2\rho_1$	A(94)	$I_\ell I_{xx}\cos^2\rho_1$
A(70)	$\cos^2\rho_1$	A(95)	$I_\ell I_{xx}\sin\rho_1\cos\rho_1$
A(71)	$\sin\rho_1\cos\rho_1$	A(96)	$I_\ell I_{xx}\sin^2\rho_1$
		A(97)	I_ℓ^2

Translational Equation Forces

The translational equation forces are as follows:

$$A(100) = F_r,$$

$$A(101) = F_A,$$

$$A(102) = F_{\phi_c}$$

The program described herein contains zeroes for these elements. Any type of force (lunar and solar perturbations, for example), which the user might desire, should be added to these elements. These forces should be evaluated in *Subroutine Deriv*.

Rotational Equation Moments and Variables

The rotational equation moments and related variables are given in Table D6. The moments are assigned to elements A(103) through A(109). The other variables are angular momentum, A(110)-A(112) and A(116); angular velocities, A(113)-A(115) and A(117)-A(125); damper rod position functions A(126) and A(127); and the inertia tensor A(128)-A(134). These are required to evaluate the moments. These calculations are made in *Subroutine Deriv*.

Momentum Transfer Terms for Collision

Table D7 relates momentum transfer terms for collisions between the vehicle body and the damper rod. This evaluation is made in *Subroutine Auto*.

Table D6
Rotational Equation Moments and Variables.

ELEMENT	PARAMETER	ELEMENT	PARAMETER	ELEMENT	PARAMETER
A(103)	M_{x_b}	A(115)	Ω_{z_d}	A(126)	$\sin^2 \rho_2$
A(104)	M_{y_b}	A(116)	$I_{\ell} \Omega_{x_d} \Omega_{y_d}$	A(127)	$\sin \rho_2 \cos \rho_2$
A(105)	M_{z_b}		$- I_{\ell} \Omega_{x_d} \dot{\rho}_2$	A(128)	K_x / Δ
A(106)	M_{x_d}	A(117)	δ_{x_b}	A(129)	K_{xy} / Δ
A(107)	M_{y_d}	A(118)	δ_{y_b}	A(130)	K_{xz} / Δ
A(108)	M_{z_d}	A(119)	δ_{z_b}	A(131)	K_y / Δ
A(109)	M_{SD}	A(120)	ξ_{x_0}	A(132)	K_{yz} / Δ
A(110)	H_{x_b}	A(121)	ξ_{y_0}	A(133)	K_z / Δ
A(111)	H_{y_b}	A(122)	ξ_{z_0}	A(134)	Δ
A(112)	H_{z_b}	A(123)	ω_{x_b}		
A(113)	Ω_{x_d}	A(124)	ω_{y_b}		
A(114)	Ω_{y_d}	A(125)	ω_{z_b}		

Table D7
Momentum Transfer Terms.

ELEMENT	PARAMETER	ELEMENT	PARAMETER
A(135)	H_{T_x}	A(140)	L_{xz}
A(136)	$H_{T_y} + (\dot{\rho}_2)_1 I_\ell \sin \rho_1$	A(141)	L_y
A(137)	$H_{T_z} - (\dot{\rho}_2)_1 I_\ell \cos \rho_1$	A(142)	L_{yz}
A(138)	L_x	A(143)	L_z
A(139)	L_{xy}	A(144)	η

Trigonometric Functions

Table D8 groups the trigonometric functions required by the program. Elements A(226) through A(231) are combinations of the previously defined trigonometric functions which are required for the gravitation moments.

Program Listing and Symbol Table

Table D9 defines alphabetic symbols which, for the most part, are used internally in the program. The FORTRAN II digital program listing is shown as Table D10.

Table D8
Trigonometric Functions.

ELEMENT	PARAMETER	ELEMENT	PARAMETER	ELEMENT	PARAMETER
A(200)	$\sin \Lambda$	A(201)	$\cos \Lambda$	A(220)	$\cos \phi \sin \psi$
A(202)	$\sin \phi_c$	A(203)	$\cos \phi_c$	A(221)	$\cos \phi \cos \psi$
A(204)	$\sin A$	A(205)	$\cos A$	A(222)	$\cos \rho_2 \cos \rho_1$
A(206)	$\sin \alpha$	A(207)	$\cos \alpha$	A(223)	$\cos \rho_2 \sin \rho_1$
A(208)	$\sin \phi$	A(209)	$\cos \phi$	A(224)	$-\sin \rho_2 \cos \rho_1$
A(210)	$\sin \psi$	A(211)	$\cos \psi$	A(225)	$-\sin \rho_2 \sin \rho_1$
A(212)	$\sin \rho_2$	A(213)	$\cos \rho_2$	A(226)	$a_1 a_2$
A(214)	$\cos \alpha \cos \phi$			A(227)	$a_1 a_3$
A(215)	$-\cos \alpha \sin \phi \sin \psi - \sin \alpha \cos \psi$			A(228)	$a_2 a_3$
A(216)	$-\cos \alpha \sin \phi \cos \psi + \sin \alpha \sin \psi$			A(229)	a_1^2
A(217)	$\sin \alpha \cos \phi$			A(230)	a_2^2
A(218)	$-\sin \alpha \sin \phi \sin \psi + \cos \alpha \cos \psi$			A(231)	a_3^2
A(219)	$-\sin \alpha \sin \phi \cos \psi - \cos \alpha \sin \psi$				

Table D9
Alphabetic Symbols.

AA	semimajor axis of the satellite orbit
AN	longitude of the ascending node of the satellite orbit
AP	argument of perigee of the satellite orbit
CAN	cosine of the longitude of the ascending node
CAP	cosine of the argument of perigee
CTHE	cosine of the true anomaly
CXI	cosine of the orbit plane inclination
ECC	eccentricity of the satellite orbit
FLAG	a storage location used to transmit the signal of a rod collision with the main body
P	semilatus rectum of the satellite orbit
PITCH	attitude angle of the satellite
RAD	conversion factor for converting radians to degrees
RHO2	angular deviation of the damper rod from equilibrium position
ROLL	attitude angle of the satellite
R2	radius vector squared
R3	earth constant divided by radius vector cubed
SAN	sine of the longitude of the ascending node
SAP	sine of the argument of perigee
STHE	sine of the true anomaly
STP	indicator of the status of calculation of momentum transfer during damper rod collision with the main body
SXI	sine of the orbit plane inclination
THE	true anomaly of the satellite in its orbit
THR	time in hours
V	total velocity
VL	longitudinal component of velocity
VP	latitudinal component of velocity
VT	vector sum of longitudinal and latitudinal components of velocity
XI	orbit plane inclination
YAW	attitude angle of the satellite
ZMU	earth's gravitation constant
ZMU3	minus three times the earth's gravitation constant

Table D10
Program Listing.

```

C   MAIN PROGRAM
      DIMENSION A(500),Y(100)
      COMMON A,Y,RAD,ZMU,ZMU3
      RAD = 57.295779
      ZMU = 1.4076449E16
      ZMU3 = -3.*ZMU
1   FORMAT(4E15.8)
2   FORMAT(1H1)
C   VEHICLE PARAMETER INPUT (TABLE D1)
      WRITE OUTPUT TAPE 3,2
      READ INPUT TAPE 2,1,A(50),A(51)
      READ INPUT TAPE 2,1,A(53),A(54),A(55)
      READ INPUT TAPE 2,1,A(59),A(60),A(61)
      READ INPUT TAPE 2,1,A(62),A(63)
      READ INPUT TAPE 2,1,A(66),A(67)
      WRITE OUTPUT TAPE 3,1,A(50),A(51)
      WRITE OUTPUT TAPE 3,1,A(53),A(54),A(55)
      WRITE OUTPUT TAPE 3,1,A(59),A(60),A(61)
      WRITE OUTPUT TAPE 3,1,A(62),A(63)
      WRITE OUTPUT TAPE 3,1,A(66),A(67)
C   CALCULATION OF CONSTANT VEHICLE INERTIA PARAMETERS (TABLE D5)
      A(52) = A(50)+A(51)
      A(56) = A(54)-A(55)
      A(57) = A(55)-A(53)
      A(58) = A(53)-A(54)
      A(65) = A(63)/RAD
      A(64) = SIN(A(65))
      A(65) = COS(A(65))
      A(68) = A(53)+A(62)
      A(69) = A(64)**2
      A(70) = A(65)**2
      A(71) = A(64)*A(65)
      A(75) = A(54)*A(55)-A(61)**2
      A(76) = A(60)*A(61)-A(55)*A(59)
      A(77) = A(59)*A(61)-A(54)*A(60)
      A(78) = A(68)*A(55)-A(60)**2
      A(79) = A(59)*A(60)-A(68)*A(61)
      A(80) = A(68)*A(54)-A(59)**2
      A(81) = A(62)*(A(54)*A(69)-2.*A(61)*A(71)+A(55)*A(70))
      A(82) = A(62)*(A(55)*A(65)-A(61)*A(64))
      A(85) = A(62)*(A(59)*A(64)-A(60)*A(65))
      A(83) = -A(85)*A(64)
      A(84) = A(62)*(A(54)*A(64)-A(61)*A(65))
      A(85) = A(85)*A(65)
      A(86) = 2.*A(62)*A(60)*A(64)
      A(87) = A(62)*(A(53)*A(69)-A(55))
      A(88) = A(62)*(-A(53)*A(71)+A(61))
      A(89) = -A(62)*(A(59)*A(64)+A(60)*A(65))
      A(90) = 2.*A(62)*A(59)*A(65)
      A(91) = A(62)*(A(53)*A(70)-A(54))
      A(92) = A(62)*(A(54)*A(70)+2.*A(61)*A(71)+A(55)*A(69))
      A(93) = -A(62)*(A(59)*A(65)+A(60)*A(64))
      A(96) = A(53)*A(62)
      A(94) = A(96)*A(70)
      A(95) = A(96)*A(71)
      A(96) = A(96)*A(69)
      A(97) = A(62)**2
C   INITIAL CONDITION AND ORBITAL ELEMENT INPUT (TABLES D2 AND D4)
C   Y(1) THRU Y(14) ARE ALL INITIALIZED
      READ INPUT TAPE 2,1,AA,ECC,XI
      READ INPUT TAPE 2,1,THE,AP,AN

```

Table D10 (Continued)

Program Listing.

```

READ INPUT TAPE 2,1,Y(7),Y(8),Y(9)
READ INPUT TAPE 2,1,Y(10),Y(11),Y(12)
READ INPUT TAPE 2,1,Y(13),Y(14)
READ INPUT TAPE 2,1,Y(15),Y(16),Y(17),Y(18)
WRITE OUTPUT TAPE 3,1,AA,ECC,XI
WRITE OUTPUT TAPE 3,1,THE,AP,AN
WRITE OUTPUT TAPE 3,1,Y(7),Y(8),Y(9)
WRITE OUTPUT TAPE 3,1,Y(10),Y(11),Y(12)
WRITE OUTPUT TAPE 3,1,Y(13),Y(14)
WRITE OUTPUT TAPE 3,1,Y(15),Y(16),Y(17),Y(18)
Y(10) = Y(10)/RAD
Y(11) = Y(11)/RAD
Y(12) = Y(12)/RAD
Y(14) = Y(14)/RAD
CTHE = THE/RAD
STHE = SIN(CTHE)
CTHE = COS(CTHE)
CAN = AN/RAD
SAN = SIN(CAN)
CAN = COS(CAN)
CXI = XI/RAD
SXI = SIN(CXI)
CXI = COS(CXI)
CAP = (THE+AP)/RAD
SAP = SIN(CAP)
CAP = COS(CAP)
A(202) = SXI*SAP
A(203) = SQRT(1.-A(202)**2)
A(204) = (SXI*CAP)/A(203)
A(205) = CXI/A(203)
A(200) = (CAN*CXI*SAP+SAN*CAP)/A(203)
A(201) = (CAN*CAP-SAN*CXI*SAP)/A(203)
P = AA*(1.-ECC**2)
Y(4) = P/(1.+ECC*CTHE)
Y(5) = ATAN(A(200),A(201))
Y(6) = ATAN(A(202),A(203))
Y(1) = SQRT(ZMU/P)*ECC*STHE
Y(3) = SQRT(ZMU*Y(4)*(1.+ECC*CTHE))
Y(2) = Y(3)*CXI
Y(3) = Y(3)*A(204)
WRITE OUTPUT TAPE 3,2
CALL RK(14)
END

```

```

SUBROUTINE RK(N)
  DIMENSION A(500),Y(100)
  COMMON A,Y,RAD,ZMU,ZMU3
  DIMENSION Y0(50),Q(50)
C  INTEGRATION INIALIZATION
  NT = N+2
  STP = 0.
  DO 1 J=1,N
1  Y0(J) = Y(J)
  T0 = T
  CALL DERIV
  CALL OUT(1)
  TPRINT = Y(N+1)+Y(N+3)

```

Table D10 (Continued)

Program Listing.

```

      GO TO 5
2 DO 3 J=1,N
3 Y0(J) = Y(J)
  TO =Y(N+1)
C   1ST STEP OF INTEGRATION
4 CALL DERIV
5 DO 6 J=1,N
  Y(J) = Y0(J)+.5*Y(NT)*A(J)
6 Q(J) = A(J)
C   2ND STEP OF INTEGRATION
  Y(N+1) = Y(N+1)+.5*Y(NT)
  CALL DERIV
  DO 7 J=1,N
    Y(J) = Y0(J)+.5*Y(NT)*A(J)
7 Q(J) = Q(J)+2.*A(J)
C   3RD STEP OF INTEGRATION
  CALL DERIV
  DO 8 J=1,N
    Y(J) = Y0(J)+Y(NT)*A(J)
8 Q(J) = Q(J)+2.*A(J)
C   4TH STEP OF INTEGRATION
  Y(N+1) = Y(N+1)+.5*Y(NT)
  CALL DERIV
  DO 9 J=1,N
    Y(J) = Y0(J)+(Y(NT)*(Q(J)+A(J)))/6.
C   CHECK POSSIBLE DAMPER ROD COLLISION
  CALL AUTO(FLAG,STP)
  IF (FLAG) 12,10,12
10 Y(N+1) = TO
  DO 11 J=1,N
11 Y(J) = Y0(J)
  GO TO 4
12 TINT = Y(N+1)-Y(N+4)
C   CHECK TERMINATION
  IF ((TINT/Y(N+4))+1.E-6) 14,13,13
C   FINAL PRINT BEFORE TERMINATION
13 CALL OUT(1)
  GO TO 18
14 IF (TINT+Y(NT)) 16,16,15
C   GET READY TO TERMINATE AFTER NEXT STEP
15 Y(NT) = -TINT
C   PRINT AND/OR PROCEED
16 IF (Y(N+1)-TPRINT) 2,17,17
17 CALL OUT(0)
  TPRINT = TPRINT+Y(N+3)
  GO TO 2
18 RETURN
  END

SUBROUTINE DERIV
  DIMENSION A(500),Y(100)
  COMMON A,Y,RAD,ZMU,ZMU3
C   TRIGONOMETRIC FUNCTIONS (TABLE D8)
  A(200) = SIN(Y(5))
  A(201) = COS(Y(5))
  A(202) = SIN(Y(6))
  A(203) = COS(Y(6))

```

Table D10 (Continued)

Program Listing.

```

VL = Y(2)/(Y(4)*A(203))
VP = Y(3)/Y(4)
A(205) = ATANF(VP,VL)
A(204) = SIN(A(205))
A(205) = COSF(A(205))
A(206) = SIN(Y(10))
A(207) = COSF(Y(10))
A(208) = SIN(Y(11))
A(209) = COSF(Y(11))
A(210) = SIN(Y(12))
A(211) = COSF(Y(12))
A(212) = SIN(Y(14))
A(213) = COSF(Y(14))
A(214) = A(207)*A(209)
A(215) = -A(207)*A(208)*A(210)-A(206)*A(211)
A(216) = -A(207)*A(208)*A(211)+A(206)*A(210)
A(217) = A(206)*A(209)
A(218) = -A(206)*A(208)*A(210)+A(207)*A(211)
A(219) = -A(206)*A(208)*A(211)-A(207)*A(210)
A(220) = A(209)*A(210)
A(221) = A(209)*A(211)
A(222) = A(213)*A(65)
A(223) = A(213)*A(64)
A(224) = -A(212)*A(65)
A(225) = -A(212)*A(64)
R2 = Y(4)**2
C A(100) THRU A(102) ARE PROVIDED TO ACCOMMODATE FORCES
C WHICH THE USER MIGHT DESIRE TO ADD TO THE PROGRAM
A(100) = 0.
A(101) = 0.
A(102) = 0.
C TRANSLATIONAL DERIVATIVES (TABLE D4)
A(1) = A(100)/A(52)+(VL**2+VP**2)/Y(4)-ZMU/R2
A(2) = (A(101)*Y(4)*A(203))/A(52)
A(3) = (A(102)*Y(4))/A(52)-(VL**2)*(A(202)/A(203))
A(4) = Y(1)
A(5) = VL/(Y(4)*A(203))
A(6) = Y(3)/R2
C TRIGONOMETRIC FUNCTIONS REQUIRED FOR GRAVITATIONAL MOMENTS
A(226) = A(214)*A(215)
A(227) = A(214)*A(216)
A(228) = A(215)*A(216)
A(229) = A(214)**2
A(230) = A(215)**2
A(231) = A(216)**2
R3 = ZMU3/(R2*Y(4))
C ANY ADDITIONAL MOMENTS THE USER MIGHT DESIRE TO ADD
C SHOULD BE INCLUDED IN A(103) THRU A(109)
A(103) = R3*(A(228)*A(56)+A(227)*A(59)-A(226)*A(60)
3+(A(231)-A(230))*A(61))
A(104) = R3*(A(227)*A(57)-A(228)*A(59)+(A(229)-A(231))*A(60)
4+A(226)*A(61))
A(105) = R3*(A(226)*A(58)+(A(230)-A(229))*A(59)+A(228)*A(60)
5-A(227)*A(61))
A(106) = 0.
A(108) = R3*A(62)*(A(214)*A(212)+A(215)*A(222)+A(216)*A(223))
A(107) = A(108)*(A(214)*A(213)+A(215)*A(224)+A(216)*A(225))
A(108) = -A(108)*(-A(215)*A(64)+A(216)*A(65))
A(109) = A(66)*Y(13)+A(67)*Y(14)
C A(110) THRU A(112) - ANGULAR MOMENTUM
A(110) = A(53)*Y(7)+A(59)*Y(8)+A(60)*Y(15)

```

Table D10 (Continued)

Program Listing.

```

A(111) = A(59)*Y(7)+A(54)*Y(8)+A(61)*Y(9)
A(112) = A(60)*Y(7)+A(61)*Y(8)+A(55)*Y(9)
C A(113) THRU A(115) - INERTIAL BODY RATES
A(113) = Y(7)*A(212)+Y(8)*A(222)+Y(9)*A(223)
A(114) = -Y(8)*A(64)+Y(9)*A(65)-Y(13)
A(115) = Y(7)*A(213)+Y(9)*A(224)+Y(9)*A(225)
C A(116) - COUPLING TERM BETWEEN ROD AND MAIN BODY
A(116) = A(62)*A(113)*(A(114)-Y(13))
C A(117) THRU A(119) - MOMENTS GROUPED TOGETHER IN
C THE ANGULAR RATE EQUATIONS (SEE EQ. 12)
A(117) = A(103)+A(106)*A(212)+A(108)*A(213)-Y(8)*A(112)
7+Y(9)*A(111)-A(116)*A(213)
A(118) = A(104)+A(106)*A(222)+A(109)*A(64)+A(108)*A(224)
8-Y(9)*A(110)+Y(7)*A(112)-A(116)*A(224)
A(119) = A(105)+A(106)*A(223)-A(109)*A(65)+A(108)*A(225)
9-Y(7)*A(111)+Y(8)*A(110)-A(116)*A(225)
C A(120) THRU A(122) - ORBITAL OR TRANSLATIONAL RATES
A(120) = (VL*A(102)-VP*A(101))/((VL**2+VP**2)*A(52))
A(121) = 0.
A(122) = A(5)*A(203)*A(205)+A(6)*A(204)
C A(123) THRU A(125) - ANGULAR RATES RELATIVE TO ORBIT
A(123) = Y(7)-A(120)*A(214)-A(122)*A(208)
A(124) = Y(8)-A(120)*A(215)-A(122)*A(220)
A(125) = Y(9)-A(120)*A(216)-A(122)*A(221)
C A(126) AND A(127) - DAMPER ROD TRIGONOMETRIC FUNCTIONS
A(126) = A(212)**2
A(127) = A(212)*A(213)
C A(128) THRU A(134) - ELEMENTS AND DETERMINANT
C OF INVERSE INERTIA MATRIX
A(128) = A(75)+A(81)*A(126)
A(129) = A(76)+A(82)*A(127)+A(83)*A(126)
A(130) = A(77)+A(84)*A(127)+A(85)*A(126)
A(134) = A(62)*A(213)
A(134) = A(128)*(A(53)+A(134)*A(213))+A(129)*(A(59)
4+A(134)*A(224))+A(130)*(A(60)+A(134)*A(225))
A(128) = A(128)/A(134)
A(129) = A(129)/A(134)
A(130) = A(130)/A(134)
A(131) = (A(78)+A(86)*A(127)+A(87)*A(126))/A(134)
A(132) = (A(79)+A(88)*A(126)+A(89)*A(127))/A(134)
A(133) = (A(80)+A(90)*A(127)+A(91)*A(126))/A(134)
C ROTATIONAL DERIVATIVES (TABLE 4)
A(7) = A(117)*A(128)+A(118)*A(129)+A(119)*A(130)
A(8) = A(117)*A(129)+A(118)*A(131)+A(119)*A(132)
A(9) = A(117)*A(130)+A(118)*A(132)+A(119)*A(133)
A(10) = (A(124)*A(210)+A(125)*A(211))/A(209)
A(11) = -A(124)*A(211)+A(125)*A(210)
A(12) = A(123)-A(10)*A(208)
A(13) = -A(8)*A(64)+A(9)*A(65)-A(113)*A(115)-(A(107)
3+A(109))/A(62)
A(14) = Y(13)
RETURN
END

```

```

SUBROUTINE AUTO(FLAG,STP)
DIMENSION A(500),Y(100)
COMMON A,Y,RAD,ZMU,ZMU3

```

Table D10 (Continued)

Program Listing.

```

      RH2 = ABSF(Y(14))
      IF (STP) 1,1,3
1  IF (RH2-1.) 7,7,2
C  SAVE OLD VALUE OF INTEGRATION TIME INTERVAL
2  DT = Y(16)
   Y(16) = Y(16)*((1.-RH1)/(RH2-RH1))
   FLAG = 0.
   STP = 2.
   GO TO 8
3  STP = STP-1.
   IF (STP) 4,4,5
C  RESTORE OLD VALUE OF INTEGRATION TIME INTERVAL
4  Y(16) = DT
   GO TO 7
5  Y(16) = DT-Y(16)
   IF (Y(13)*Y(14)) 7,7,6
C  MOMENTUM TRANSFER (TABLE D7)
6  A(135) = A(110)+A(62)*A(115)*A(213)
   A(136) = A(111)-A(62)*(A(114)*A(64)-A(115)*A(224)-Y(13)*A(64))
   A(137) = A(112)+A(62)*(A(114)*A(65)+A(115)*A(225)-Y(13)*A(65))
   A(138) = A(128)*A(134)+A(97)*A(126)+A(92)
   A(139) = A(129)*A(134)+A(97)*A(222)*A(212)+A(93)*A(65)
   A(140) = A(130)*A(134)+A(97)*A(223)*A(212)+A(93)*A(64)
   A(144) = A(62)*A(213)
   A(144) = A(138)*(A(53)+A(144)*A(213))+A(139)*(A(59)
4+A(144)*A(224))+A(140)*(A(60)+A(144)*A(225))
4+A(140)*(A(60)+A(144)*A(225))
   A(138) = A(138)/A(144)
   A(139) = A(139)/A(144)
   A(140) = A(140)/A(144)
   A(141) = (A(131)*A(134)+A(94)+A(97)*A(222)**2)/A(144)
   A(142) = (A(132)*A(134)+A(95)+A(97)*A(222)*A(223))/A(144)
   A(143) = (A(133)*A(134)+A(96)+A(97)*A(223)**2)/A(144)
   Y(7) = A(135)*A(138)+A(136)*A(139)+A(137)*A(140)
   Y(8) = A(135)*A(139)+A(136)*A(141)+A(137)*A(142)
   Y(9) = A(135)*A(140)+A(136)*A(142)+A(137)*A(143)
20 FORMAT(8X13H HIT STOP AT E11.4, 8H RAD/SEC)
   WRITE OUTPUT TAPE 3,20,Y(13)
   Y(13) = -Y(13)
7  RH1 = RH2
   FLAG = 1.
8  RETURN
   END

```

```

      SUBROUTINE OUT(K)
      DIMENSION A(500),Y(100)
      COMMON A,Y,RAD,ZMU,ZMU3
      THR = Y(15)/3600.
      PITCH = Y(10)*RAD
      ROLL = Y(11)*RAD
      YAW = Y(12)*RAD
      INT = YAW/360.
      XINT = INT
      YAW = YAW-XINT*360.
      RH02 = Y(14)*RAD
C  TEST OUTPUT MODE
   IF (K) 1,1,2

```

Table D10 (Continued)

Program Listing.

```

C   OUTPUT MODE (0)   (TABLE D3)
1  WRITE OUTPUT TAPE 3,20,THR,PITCH,ROLL,YAW,RHO2
20 FORMAT(5F12.4)
   GO TO 9
2  CXI = A(203)*A(205)
   SXI = SQRTF(1.-CXI**2)
   XI = ATANF(SXI,CXI)*RAD
   IF (XI) 3,4,3
3  SAN = A(200)*A(204)-A(201)*A(202)*A(205)
   CAN = A(201)*A(204)+A(200)*A(202)*A(205)
   AN = ATANF(SAN,CAN)*RAD
   CAP = A(203)*A(204)
   AP = ATANF(A(202),CAP)*RAD
   GO TO 5
4  AN = 0.
   AP = ATANF(A(200),A(201))*RAD
5  VL = Y(2)/(Y(4)*A(203))
   VP = Y(3)/Y(4)
   VT = VL**2+VP**2
   V = Y(1)**2+VT
   Q = (Y(4)*V)/ZMU
   CL2 = VT/V
   AA = Y(4)/(2.-Q)
   ECC = SQRTF(1.-Q*(2.-Q)*CL2)
   IF (ECC-1.E-5) 7,7,6
6  CTHE = SQRTF(VT)-SQRTF(ZMU/(AA*(1.-ECC**2)))
   THE = ATANF(Y(1),CTHE)*RAD
   AP = AP-THE
   GO TO 8
7  THE = AP
   AP = 0.
   ECC = 0.
8  V = SQRTF(V)
C   OUTPUT MODE (1)   (TABLE D3)
   WRITE OUTPUT TAPE 3,23
   WRITE OUTPUT TAPE 3,21,THR,Y(15)
   WRITE OUTPUT TAPE 3,22,PITCH,Y(7),AA,THE
   WRITE OUTPUT TAPE 3,22,ROLL,Y(8),ECC,AP
   WRITE OUTPUT TAPE 3,22,YAW,Y(9),XI,AN
   WRITE OUTPUT TAPE 3,21,Y(4),V,RHO2,Y(13)
   WRITE OUTPUT TAPE 3,23
21 FORMAT(4E18.8)
22 FORMAT(E20.8,3E18.8)
23 FORMAT(1H0)
9  RETURN
   END

```